

1 **Mutations in *HUA2* restore flowering in the *Arabidopsis trehalose***
2 ***6-phosphate synthase1 (tps1)* mutant**
3

4 **Liping Zeng^{1,2,*}, Vasiliki Zacharaki³, Yanwei Wang¹, Markus Schmid^{1,3,4,*}**

5
6 ¹ Beijing Advanced Innovation Centre for Tree Breeding by Molecular Design, College of
7 Biological Sciences and Biotechnology, Beijing Forestry University, Beijing 100083,
8 People's Republic of China.

9 ² School of Grassland Science, Beijing Forestry University, Beijing 100083, People's
10 Republic of China.

11 ³ Umeå Plant Science Centre, Department of Plant Physiology, Umeå University, SE-901 87
12 Umeå, Sweden.

13 ⁴ Department of Plant Biology, Linnean Center for Plant Biology, Swedish University of
14 Agricultural Sciences, S-75007 Uppsala, Sweden.

15
16 * Corresponding author(s)

17
18 **Author emails and ORCID:**

19 zenglp2020@163.com (0009-0005-3691-1505)
20 vasiliki.zacharaki@umu.se (0000-0002-5543-2332)
21 ywwang@bjfu.edu.cn (0000-0002-4111-4843)
22 markus.schmid@slu.se (0000-0002-0068-2967)

23
24 **Short title:** *hua2* represses *tps1* mutation

25
26 **Authors responsible for distribution of materials:**

27 Liping Zeng (zenglp2020@163.com) and Markus Schmid (markus.schmid@slu.se)

28 **Abstract**

29 Plant growth and development are regulated by many factors, including carbohydrate
30 availability and signaling. Trehalose 6-phosphate (T6P), which is synthesized by
31 TREHALOSE-6-PHOSPHATE SYNTHASE 1 (TPS1), is positively correlated with and
32 functions as a signal that informs the cell about the carbohydrate status. Mutations in *TPS1*
33 negatively affect the growth and development of *Arabidopsis thaliana* and complete
34 loss-of-function alleles are embryo lethal, which can be overcome using inducible expression
35 of *TPS1* (*GVG::TPS1*) during embryogenesis. Using EMS mutagenesis in combination with
36 genome re-sequencing we have identified several alleles in the floral regulator *HUA2* that
37 restore flowering and embryogenesis in *tps1-2 GVG::TPS1*. Genetic analyses using a *HUA2*
38 T-DNA insertion allele, *hua2-4*, confirmed this finding. RNA-seq analyses demonstrated that
39 *hua2-4* has widespread effects on the *tps1-2 GVG::TPS1* transcriptome, including key genes
40 and pathways involved in regulating flowering. Higher order mutants combining *tps1-2*
41 *GVG::TPS1* and *hua2-4* with alleles in the key flowering time regulators *FLOWERING*
42 *LOCUS T (FT)*, *SUPPRESSOR OF OVEREXPRESSION OF CONSTANS 1 (SOC1)*, and
43 *FLOWERING LOCUS C (FLC)* were constructed to analyze the role of *HUA2* during floral
44 transition in *tps1-2* in more detail. Taken together, our findings demonstrate that loss of
45 *HUA2* can restore flowering and embryogenesis in *tps1-2 GVG::TPS1* in part through
46 activation of *FT*, with contributions of the upstream regulators *SOC1* and *FLC*. Interestingly,
47 we found that mutation of *FLC* is sufficient to induce flowering in *tps1-2 GVG::TPS1*.
48 Furthermore, we observed that mutations in *HUA2* modulate carbohydrate signaling and that
49 this regulation might contribute to flowering in *hua2-4 tps1-2 GVG::TPS1*.

50

51 **Keywords:** carbohydrate signaling, Trehalose 6-phosphate (T6P), *TREHALOSE*
52 *PHOSPHATE SYNTHASE1 (TPS1)*, *HUA2*, Flowering time, *Arabidopsis thaliana*

53 **Introduction**

54 Plants have evolved intricate signaling mechanisms that enable them to monitor a wide range
55 of environmental and endogenous cues and adjust their physiology, growth, and development
56 accordingly. Adjustments occur more or less constantly, but developmental phase transitions
57 such as germination, the switch from juvenile to adult growth, or the induction of flowering
58 and reproductive development are under particularly stringent control.

59 In *Arabidopsis thaliana*, the floral transition is controlled by environmental factors including
60 exposure to prolonged periods of cold (vernalization), ambient temperature, day length
61 (photoperiod), light quality, and endogenous signals such as plant age, diverse hormones
62 including gibberellic acid (GA), and carbohydrate signaling (Srikanth and Schmid, 2011;
63 Romera-Branchat et al., 2014; Cho et al., 2017). Eventually, these signaling pathways
64 converge on and regulate the expression of key floral integrator genes such as *FLOWERING*
65 *LOCUS T (FT)* and *SUPPRESSOR OF OVEREXPRESSION OF CONSTANS 1 (SOC1)*
66 (Kardailsky et al., 1999; Moon et al., 2005; Kobayashi and Weigel, 2007; Turck et al., 2008;
67 Lee and Lee, 2010; Jung et al., 2012). *FT* is induced in response to permissive photoperiod in
68 the leaf vasculature where it is also translated. The *FT* protein is then transported via the
69 phloem to the shoot apical meristem (SAM) where it interacts with the bZIP transcription
70 factor FD and 14-3-3 proteins to form the florigen activation complex (FAC) (Abe et al.,
71 2005; Wigge et al., 2005; Mathieu et al., 2007; Taoka et al., 2011; Collani et al., 2019). In
72 contrast, *SOC1* is induced and acts largely at the SAM, both downstream and in parallel to *FT*
73 (Yoo et al., 2005; Lee and Lee, 2010). Eventually, these factors induce flower meristem
74 identity genes such as *LEAFY (LFY)* and *APETALA1 (API)* at the SAM, thus completing the
75 floral transition (Weigel and Nilsson, 1995; Liljegren et al., 1999; Blázquez and Weigel,
76 2000).

77 Apart from photoperiod, carbohydrate signaling has been shown to be necessary for *FT*
78 expression (Wahl et al., 2013). Sucrose is the major product of photosynthesis and most
79 common transport-sugar. However, rather than measuring sucrose concentration directly,
80 plants employ trehalose 6-phosphate (T6P) as a readout and signal of sucrose availability
81 (Goddijn and van Dun, 1999; Lunn et al., 2006; Martins et al., 2013; Yadav et al., 2014;

82 Figueroa and Lunn, 2016). T6P is the intermediate of trehalose synthesis. It is synthesized
83 from glucose 6-phosphate and uridine diphosphate glucose by TREHALOSE
84 6-PHOSPHATE SYNTHASE (TPS) and subsequently dephosphorylated by TREHALOSE
85 6-PHOSPHATE PHOSPHATASE (TPP) (Cabib and Leloir, 1958).

86 In *Arabidopsis thaliana*, there are 11 *TPS* genes (*AtTPS1*–*AtTPS11*), which can be divided
87 into two subclades, class I and class II, and 10 *TPP* genes (*TPPA*–*TPPJ*) (Leyman et al., 2001;
88 Lunn, 2007; Vandesteene et al., 2012). Of the class I *TPS* genes (*AtTPS1*–*AtTPS4*), only
89 *AtTPS1*, *AtTPS2*, and *AtTPS4* have demonstrable catalytic activity, whereas *AtTPS3* harbors a
90 premature translational stop codon and is likely a pseudogene (Blázquez et al., 1998; Van
91 Dijck et al., 2002; Lunn, 2007; Delorge et al., 2015). Class II *TPS* genes (*AtTPS5*–*AtTPS11*),
92 for which no TPS activity, has been detected, which have been reported to participate in cell
93 size regulation, thermotolerance, and cold and salt resistance, but the underlying molecular
94 mechanisms remain largely unclear (Chary et al., 2008; Ramon et al., 2009; Singh et al., 2011;
95 Tian et al., 2019; Van Leene et al., 2022). The main T6P synthase in *Arabidopsis thaliana* is
96 *TPS1*. *TPS1* loss-of-function mutants are embryonic lethal (Eastmond et al., 2002), but
97 homozygous *tps1-2* mutants could be established by dexamethasone-inducible expression of
98 *TPS1* (*GVG::TPS1*) during embryogenesis (van Dijken et al., 2004). Interestingly, the
99 resulting homozygous *tps1-2* *GVG::TPS1* plants flower extremely late compared to wild type
100 under both short- and long-day conditions. At the molecular level, late flowering of *tps1-2*
101 *GVG::TPS1* has been attributed to the combined misregulation of key flowering time genes.
102 In particular, *tps1-2* *GVG::TPS1* mutant plants fail to induce *FT* in leaves even under
103 permissive photoperiod. In addition, *MIR156* and its targets, the *SQUAMOSA PROMOTER*
104 *BINDING PROTEIN LIKE* (*SPL*) genes, which together constitute the age pathway, are also
105 misregulated in *tps1-2* *GVG::TPS1* (Wahl et al., 2013). Nevertheless, many questions
106 regarding the regulation of plant growth and development by the T6P pathway remain open.
107 In an EMS suppressor screen, we have recently reported dozens of mutations that partially
108 restored flowering and seed set in *tps1-2* *GVG::TPS1*, including several alleles in *SNF1*
109 *KINASE HOMOLOG 10* (*KIN10*) and *HOMOLOG OF YEAST SUCROSE*
110 *NONFERMENTING 4* (*SNF4*), two subunits of *Arabidopsis thaliana SNF1-Related Kinase 1*

111 (*SnRK1*) (Jung et al., 2012; Zacharaki et al., 2022), an evolutionary conserved regulator of
112 cellular energy homeostasis.

113 Here, we identified several new alleles in *HUA2* (*At5g23150*) that partially rescue the *tps1-2*
114 *GVG::TPS1* phenotype. Mutations in *HUA2* were originally identified in a genetic screen as
115 enhancers of the *AGAMOUS* (*AG*) allele *ag-4* (Chen and Meyerowitz, 1999). In addition,
116 *HUA2* has also been reported to affect shoot morphology and function as a repressor of
117 flowering (Doyle et al., 2005; Wang et al., 2007). At the molecular level, *HUA2* has been
118 suggested to function as a putative transcription factor but has also been implicated in RNA
119 processing (Cheng et al., 2003). We show that three different EMS-induced point mutations
120 in *HUA2* restore flowering in *tps1-2 GVG::TPS1* and verify this finding using a previously
121 described T-DNA insertion allele, *hua2-4*. RNA-seq analyses revealed widespread effects of
122 *hua2-4* on the *tps1 GVG::TPS1* transcriptome, including activation of flower integrator genes
123 such as *SOC1* and *AGAMOUS-LIKE 24* (*AGL24*). Genetic analyses demonstrated that
124 induction of flowering in *tps1-2 GVG::TPS1* required functional *FT*. Furthermore, we
125 observed that loss of *FLOWERING LOCUS C* (*FLC*) is sufficient to induce flowering in
126 *tps1-2 GVG::TPS1*. Interestingly, *hua2-4* also attenuated the induction of known *SnRK1*
127 target genes in response to carbon starvation. Taken together, our results identify mutations in
128 *HUA2* as suppressors of the non-flowering phenotype of *tps1-2 GVG::TPS1* and provide
129 insights into the underlying genetic and molecular pathways.

130

131 **Results**

132 **Mutations in *hua2* restore flowering in *tps1-2 GVG::TPS1***

133 To identify novel components of the T6P pathway, we recently conducted a suppressor screen
134 in which the non-flowering *tps1-2 GVG::TPS1* mutant was subjected to ethyl methane
135 sulfonate (EMS) mutagenesis. In total, 106 M2 mutant plants in which flowering and seed set
136 was at least partially restored were isolated, and EMS-induced SNPs were identified by
137 whole genome sequencing in a subset of 65 mutants (Zacharaki et al., 2022). To identify

138 additional candidate suppressor genes in which SNPs were overrepresented, we expanded this
139 list to 92 by sequencing the genomes of another 27 mutants (Table S1).

140 Analysis of these 92 genome sequences for genes with multiple independent EMS-induced
141 mutations identified three SNPs in the coding sequence of *HUA2* (*AT5G23150*) (Table S2,
142 S3). The three alleles result in non-synonymous amino acid substitutions, namely A983T,
143 P455S, and R902C. We refer to these new EMS-induced suppressor lines as *hua2-11* (line
144 #8-1-1), *hua2-12* (line #233-14-1), and *hua2-13* (line #164-9-1), respectively (Fig. 1A). The
145 polymorphism R902C resides at the C-terminal end of the HUA2 CID motif (RNA Pol-II
146 C-terminal domain (CTD) interaction domain). The *hua2-11* (line #8-1-1) allele was also
147 detected in two additional suppressor lines, #57-2-1 and #30-34 (Table S2, S3). As these
148 three lines share most EMS-induced SNPs genome-wide, we assume these lines originate
149 from the same parental plant.

150 Importantly, flowering was restored in all three *hua2* alleles, even though all three mutant
151 lines produced substantially more leaves before making the transition to flowering than Col-0
152 control plants (Fig. 1B, C). The flowering time of *hua2-11* was 32.15 days, whereas *hua2-12*
153 and *hua2-13* flowered after 46.5 and 50.9 days, respectively, compared to Col-0, which
154 flowered after 25.2 days. Thus, the three mutants form an allelic series with *hua2-11* being
155 the strongest and *hua2-13* being the weakest allele. As *HUA2* has previously been implicated
156 in flowering time regulation and has been shown to regulate the expression of a group of
157 MADS-box transcription factors known to form a floral repressive complex in *Arabidopsis*
158 *thaliana* (Doyle et al., 2005; Wang et al., 2007; Lee et al., 2013; Posé et al., 2013; Jali et al.,
159 2014; Yan et al., 2016), we considered mutations in this gene as likely to be causal for the
160 restoration of flowering in the *tps1-2 GVG::TPS1* suppressor lines.

161 Since the three *hua2* alleles described above were generated through EMS mutagenesis, it is
162 possible that other independent mutations not linked to *HUA2* could be involved in partially
163 rescuing the *tps1-2 GVG::TPS1* phenotype. To confirm that mutations in *HUA2* are causal for
164 the suppression of the *tps1-2* non-flowering phenotype, we crossed *tps1-2 GVG::TPS1* with
165 *hua2-4*, a previously described *hua2* loss-of-function mutant that carries a T-DNA insertion
166 in the 2nd intron (Fig. 2A) (Doyle et al., 2005). Of the F2 plants homozygous for the *tps1-2*

167 mutations, only those approx. 25% that were homozygous for the *hua2-4* T-DNA insertion
168 flowered without application of dexamethasone. Similar to *hua2-11 tps1-2 GVG::TPS1* (Fig.
169 1B,C), *hua2-4 tps1-2 GVG::TPS1* double mutants displayed a bushy shoot phenotype and
170 were moderately late flowering (Fig. 2B,C). Taken together, our findings confirm that
171 recessive mutations in *HUA2* are responsible for the induction of flowering in *tps1-2*
172 *GVG::TPS1*. Our findings also suggest that *HUA2* normally functions by repressing
173 flowering either directly or indirectly through the promotion of floral repressors.

174 ***hua2-4* has widespread effects on the *tps1-2 GVG::TPS1* transcriptome**

175 To identify possible downstream targets of *HUA2* whose misexpression might explain the
176 induction of flowering in the suppressor mutant, we performed RNA-seq analysis in leaves of
177 21-d-old *tps1-2 GVG::TPS1* plants, *tps1-2 GVG::TPS1* plants treated with dexamethasone,
178 and the *hua2-4 tps1-2 GVG::TPS1* double mutant. Plants were grown under long days (16 h
179 light, 8 h dark) in the presence or absence of dexamethasone and samples were collected at
180 ZT4 (Zeitgeber time 4, means 4 h after lights on). Genes that were differentially expressed in
181 three independent replicates per genotype and treatment were identified using Cuffdiff.

182 We observed that dexamethasone treatment significantly affected the expression of 9600
183 genes in *tps1-2 GVG::TPS1*. Of these, 4830 and 4770 genes were upregulated and
184 downregulated, respectively (Fig. 3A). In contrast, mutation of *hua2* affected the expression
185 of only 2066 genes, of which 988 and 1078 genes were upregulated and downregulated in
186 *hua2-4 tps1-2 GVG::TPS1*, respectively (Fig. 3A). In total our RNA-seq analysis identified
187 1437 genes that are differentially expressed in *tps1-2 GVG::TPS1* in response to
188 dexamethasone application and the *hua2-4* mutation. Importantly, *HUA2* expression is not
189 changed in *tps1-2 GVG::TPS1* in response to dexamethasone application, suggesting that
190 *hua2* might induce flowering largely by activating a pathway not normally regulated by the
191 T6P pathway (Fig. S1).

192 Since both, dexamethasone application and mutations in *hua2* can induce flowering in *tps1-2*
193 *GVG::TPS1*, we next searched for genes that were repressed or induced in response to either
194 treatment. We identified 412 genes that were downregulated in *tps1-2 GVG::TPS1* in

195 response to dexamethasone application and mutations in *hua2* (Fig. 3A). Gene ontology (GO)
196 analysis revealed that among others, processes such as flavonoid metabolism (GO:0009812),
197 carbohydrate transport (GO:0008643), and starvation response (GO:0009267) were
198 significantly enriched, which is in line with the well-established role of *TPS1* in remodeling
199 carbohydrate metabolism (Fig. 3B; Table S4).

200 In addition, we identified 243 genes that were induced in response to dexamethasone and in
201 *hua2-4 tps1-2 GVG::TPS1*. Among these genes, GO categories related to the response to
202 gibberellin (GO:0009739) and the regulation of timing of meristematic phase transition
203 (GO:0048506) are of particular interest as they are directly linked to the transition to
204 flowering (Fig. 3C; Table S5). Importantly, among the genes induced in *tps1-2 GVG::TPS1*
205 by dexamethasone and *hua2* were *SUPPRESSOR OF OVEREXPRESSION OF CONSTANS 1*
206 (*SOC1*) and *AGAMOUS-LIKE 24* (*AGL24*), two MADS-domain transcription factors known
207 to promote the transition to flowering (Fig. 3D; Table S6). In contrast, other known flowering
208 time regulators such as *CONSTANS* (*CO*), *FT*, and *TWIN SISTER OF FT* (*TSF*) are either
209 hardly detectable (Fig. S2A), possibly because of the collection time of the RNA-seq samples
210 at ZT 4 or did not change significantly in *hua2* and in response to dexamethasone treatment
211 (Fig. S2B). In summary, our transcriptome analysis identified several downstream genes and
212 pathways whose misregulation could contribute to the induction of flowering in *tps1-2*
213 *GVG::TPS1* in response to dexamethasone application or loss of *hua2* (Fig. S2; Table S6).

214 **Induction of flowering of *tps1-2 GVG::TPS1* by *hua2-4* requires *FT***

215 To test whether *SOC1*, which we found to be differentially expressed in response to
216 dexamethasone application or in *hua2-4 tps1-2 GVG::TPS1*, is a major target of *HUA2* in the
217 regulation of flowering time in *tps1-2 GVG::TPS1* we constructed the *soc1-2 hua2-4 tps1-2*
218 *GVG::TPS1* triple mutant. We observed that the triple mutant flowered only moderately later
219 than the *hua2-4 tps1-2 GVG::TPS1* double mutant (Fig. 4A,B). This indicates that even
220 though *SOC1* is significantly induced in our RNA-seq experiment in *hua2-4 tps1-2*
221 *GVG::TPS1* (Fig. 3D; Table S6) and in RT-qPCR experiments (Fig. 4C), *SOC1* is largely
222 dispensable for the induction of flowering in *tps1-2 GVG::TPS1* by loss of *hua2*.

223 SOC1 is known to act partially upstream of the flowering time integrator gene and florigen
224 FT. We, therefore, decided to test if induction of flowering in *tps1-2 GVG::TPS1* by *hua2-4*
225 required functional *FT*. Interestingly, mutation of *FT* completely abolished the effect of
226 *hua2-4* on flowering of *tps1-2 GVG::TPS1* and the *ft-10 hua2-4 tps1-2 GVG::TPS1* triple
227 mutant failed to flower even after four months of growth in inductive long-day conditions
228 (Fig. 4D,E). In line with this observation, we detected increased expression of *FT* at the end
229 of the long day (ZT 16) in the *hua2-4 tps1-2 GVG::TPS1* double mutant when compared to
230 *tps1-2 GVG::TPS1* (Fig. 4F). It is interesting to note that *FT* expression was barely detectable
231 at ZT 4 according to our RNA-seq analysis (Fig. S2A), which is in agreement with the
232 diurnal expression pattern reported for *FT* (Kobayashi et al., 1999). Taken together, our
233 genetic and molecular analyses indicate that *hua2-4* induces flowering of *tps1-2 GVG::TPS1*
234 in part through activation of *FT*, with minor contributions of the upstream regulators *SOC1*.

235 **Loss of *FLC* induces flowering in *tps1-2 GVG::TPS1***

236 *HUA2* has previously been reported to regulate flowering at least in part by regulating the
237 expression of floral repressors of the MADS-domain transcription factor family, including
238 *FLOWERING LOCUS C (FLC)* and *FLOWERING LOCUS M (FLM)* (Doyle et al., 2005). To
239 test if *hua2-4* induces flowering in *tps1-2 GVG::TPS1* through these repressors we constructed
240 the *flc-3 hua2-4 tps1-2 GVG::TPS1* triple mutant. We found that this triple mutant flowered
241 moderately earlier than *hua2-4 tps1-2 GVG::TPS1* (Fig. 4G,H). In agreement with these
242 findings, RT-qPCR analysis failed to detect *FLC* expression in the *hua2-4 tps1-2 GVG::TPS1*
243 mutant, whereas *FLC* expression was readily detectable by RT-qPCR in *tps1-2 GVG::TPS1*
244 (Fig. 4I).

245 Furthermore, we found that the expression of *FLC* was significantly upregulated in
246 18-day-old *tps1-2 GVG::TPS1* seedlings when compared to Col-0 in publicly available
247 RNA-seq data (Zacharaki et al., 2022) (Fig. 5A). This prompted us to test loss of *FLC* on its
248 own might be sufficient to suppress the non-flowering phenotype of *tps1-2 GVG::TPS1*.
249 Indeed, we observed that *flc-3* alone is capable of inducing flowering in the otherwise
250 non-flowering *tps1-2 GVG::TPS1* mutant background, even though the *flc-3 tps1-2*
251 *GVG::TPS1* double mutant flowered significantly later than wild-type and *flc-3* (Fig. 5B,C).

252 These findings suggest that the failure of *tps1-2 GVG::TPS1* to flower could in part be due to
253 *FLC*, possibly in conjunction with other MADS-box repressors such as *MADS AFFECTING*
254 *FLOWERING 5 (MAF5)*, the expression of which was also elevated in *tps1-2 GVG::TPS1*
255 (Fig. 5A). In contrast, expression of *HUA2* was not changed in *tps1-2 GVG::TPS1* when
256 compared to Col-0 according to publicly available RNA-seq data (Fig. S3).

257 ***hua2-4* attenuates carbon starvation responses**

258 The above data indicate that mutations in *HUA2* bypass the requirement for *TPS1* to induce
259 flowering by reducing expression of MADS-box floral repressors and ultimately inducing
260 floral integrator genes such as *FT* and *SOC1*. However, carbohydrate signaling has been
261 shown to also indirectly regulate phase transitions, including flowering, in *A. thaliana*
262 (Corbesier et al., 1998; Gibson, 2005; Xing et al., 2015; Wang et al., 2020). In part, this
263 response is mediated by SnRK1, which in response to stress conditions such as extended
264 darkness phosphorylates a range of proteins, including several C- and S1-class bZIP
265 transcription factors. Activation of these transcription factors by SnRK1 induces expression
266 of stress response genes, including *SENESCENCE5 (SEN5)* and *DARK*
267 *INDUCED6/ASPARAGINE SYNTHASE1 (DIN6/ASN1)*, which can be used as a proxy for
268 SnRK1 activity (Delatte et al., 2011; Dietrich et al., 2011; Mair et al., 2015). To test if loss of
269 *HUA2* might affect flowering also more indirectly by modulating cellular energy responses,
270 we analyzed the expression of *SEN5* and *DIN6*. Interestingly, we found that induction of
271 *SEN5* and *DIN6* in response to extended night was strongly attenuated in *hua2-4* (Fig. 6A, B)
272 similar to what we had previously observed in mutants affected in SnRK1 subunits
273 (Zacharaki et al., 2022). This finding indicates that mutations in *HUA2* might modulate
274 carbohydrate signaling more directly and that this regulation might contribute to the induction
275 of flowering in *hua2-4 tps1-2 GVG::TPS1*. In agreement with this hypothesis, we found that
276 expression of *SEN5* and *DIN6* was even further attenuated in three independent *hua2-4 tps1-2*
277 *GVG::TPS1* lines (Fig. 6A,B).

278

279 **Discussion**

280 *Arabidopsis thaliana HUA2* has been reported to play a crucial role in various aspects of
281 plant growth and development. *HUA2* was initially identified as an enhancer of the
282 *AGAMOUS* (*AG*) allele *ag-4* (Chen and Meyerowitz, 1999). Later, *HUA2* was found to also
283 play a role as a repressor of flowering (Doyle et al., 2005; Wang et al., 2007). At the
284 molecular level, *HUA2* has been suggested to function as a putative transcription factor but
285 has also been implicated in RNA processing (Cheng et al., 2003). *HUA2* is expressed
286 throughout the whole plant growth period (Chen and Meyerowitz, 1999), indicating the
287 importance and widespread effects on plant growth. Here, our study showed that loss of
288 *HUA2* can partially restore flowering and embryogenesis in *tps1-2 GVG::TPS1*.

289 It is interesting to note that in our EMS suppressor screen, we did not identify mutations in
290 any of the *HUA2-like* genes, *HULK1*, *HULK2*, and *HUL3*, present in *A. thaliana* (Jali et al.,
291 2014). One possible explanation is that our genetic screen might not have been saturated or
292 that *HUA2-like* genes were missed due to the relatively low sequencing coverage. However,
293 we believe this to be rather unlikely given that our approach has recovered multiple alleles in
294 *HUA2* (this study) as well as two SnRK1 subunits (Zacharaki et al., 2022). Furthermore,
295 flowering time is unaffected in the *hua2-like* single mutants and *hulk2 hulk3* double mutants
296 have been shown to be late flowering (Jali et al., 2014). Thus, it seems unlikely that mutation
297 in any of the *HUA2-like* genes would suppress the non-flowering phenotype of *tps1-2*
298 *GVG::TPS1*.

299 *HUA2* has been reported to exert its function in part by regulating the expression of
300 MADS-box transcription factors (Doyle et al., 2005), named after *MINICHROMOSOME*
301 *MAINTENANCE 1* (*MCM1*) in yeast, *AGAMOUS* (*AG*) in *Arabidopsis*, *DEFICIENS* (*DEF*)
302 in *Antirrhinum*, and serum response factor (SRF) in humans. MADS-BOX domain
303 transcription factors contribute to all major aspects of the life of land plants, such as female
304 gametophyte, floral organ identity, seed development, and flowering time control (Portereiko
305 et al., 2006; Colombo et al., 2008; Koo et al., 2010; Lee et al., 2013; Posé et al., 2013). In this
306 context, it is interesting to note that our transcriptome and genetic analysis identified several
307 MADS-box transcription factors to be misregulated in *tps1-2 GVG::TPS1*. In particular, the
308 well-known floral repressors *FLOWERING LOCUS C* (*FLC*) and *MADS AFFECTING*

309 *FLOWERING5 (MAF5)* were found to be induced in *tps1-2 GVG::TPS1* compared to Col-0
310 (Fig. 5A). Moreover, loss of *FLC* was sufficient to induce flowering in *tps1-2 GVG::TPS1*
311 (Fig. 5B,C), suggesting that these floral repressors are partially responsible for the
312 non-flowering phenotype of *tps1-2 GVG::TPS1*. Our transcriptome analyses further identified
313 two MADS-box transcription factors, *SUPPRESSOR OF OVEREXPRESSION OF*
314 *CONSTANS 1 (SOC1)* and *AGAMOUS-LIKE 24 (AGL24)*, both known to promote flowering
315 in *Arabidopsis*, to be upregulated in *hua2-4 tps1-2 GVG::TPS1*.

316 The molecular mechanism by which *HUA2* regulates the expression of these MADS-box
317 flowering time regulators is currently unclear. However, since *HUA2* localizes to the nucleus,
318 it seems possible that *HUA2* is directly involved in regulating the expression of these genes.
319 For example, *HUA2* could (directly) promote the expression of *FLC*, which has previously
320 been shown to directly bind to and repress the expression of *FT* and *SOC1* (Chen and
321 Meyerowitz, 1999; Doyle et al., 2005; Deng et al., 2011). In such a scenario, the increased
322 expression of *FT*, *SOC1*, and *AGL24* in *hua2-4 tps1-2 GVG::TPS1* would be the result of
323 reduced expression of floral repressors such as *FLC* and *MAF5*. However, the regulation of
324 flowering is a very complex process full of intricate feedback loops and *HUA2* might regulate
325 *SOC1* and *AGL24* directly, rather than indirectly. In this context, it is interesting to note that a
326 nonfunctional *hua2* allele may compensate for the loss of *FLC* in *Ler* accession (Lemus et al.,
327 2023). Alternatively, *HUA2* might affect the expression of these important flowering time
328 genes through interaction with RNA Pol-II via its CID domain, which is affected by the
329 *hua2-13* alleles (R902C). Interestingly, polymorphisms resulting in amino acid substitutions
330 in natural accessions of *A. thaliana* have been reported for R902 and A983, but not for P455
331 (The 1001 Genomes Consortium, 2016). Even though the molecular mechanisms underlying
332 *HUA2* function remain elusive, our results confirm *HUA2* as a central regulator of flowering
333 time in *Arabidopsis thaliana*.

334 We have previously identified mutations in two subunits of *SNF1-Related Kinase 1 (SnRK1)*,
335 *KIN10* and *SNF4*, that partially restore flowering and seed set in *tps1-2 GVG::TPS1*
336 (Zacharaki et al., 2022). Identification of these suppressor mutations was in line with the role
337 of SnRK1 as a downstream regulator of the T6P pathway and other stresses. Antagonizing

338 SnRK1 in the regulation of energy homeostasis in plants is target of rapamycin (TOR), the
339 activity of which is inhibited under energy-limiting conditions (Baena-González and Hanson,
340 2017; Belda-Palazón et al., 2022). In contrast to mutations in *KIN10* and *SNF4*, mutations in
341 *HUA2* appear, at first glance, to be bypass mutations that induce flowering independently of
342 T6P signaling. However, and rather unexpectedly, we did observe that mutation of *HUA2*
343 attenuated the induction of the carbon starvation markers *SEN5* and *DIN6* in response to
344 extended night treatments (Fig. 6A, B), indicating that mutations in *HUA2* might modulate
345 carbohydrate signaling more directly than anticipated. How exactly *HUA2* modulates carbon
346 responses in *Arabidopsis* remains to be established. It is well-known that T6P signaling
347 through *SnRK1* affects processes such as carbon starvation response, germination, flowering,
348 and senescence in opposition to the TOR (target of rapamycin) pathway (Figueroa and Lunn,
349 2016; Baena-González and Lunn, 2020). The regulatory network controlling this central
350 metabolic hub is still not fully understood and new players are constantly added. For example,
351 it has recently been shown that class II TPS proteins are important negative regulators of
352 *SnRK1* (Van Leene et al., 2022).

353 Regarding a possible role of *HUA2* in integrating carbon responses, it is worth noting that
354 flavonoid-related genes (GO:0009812) were downregulated in *tps1-2 GVG::TPS1* in
355 response to dexamethasone application and the *hua2* mutant (Fig. 3B). This is interesting as
356 *HUA2* is known to promote anthocyanin accumulation (Ilk et al., 2015), whereas *SnRK1* has
357 been shown to repress sucrose-induced anthocyanin production (Li et al., 2014; Meng et al.,
358 2018; Brouke et al., 2023). Thus, *HUA2* might constitute an important hub in coordinating
359 metabolic responses. However, as expression of *SnRK1* subunits is not affected in *hua2-4*
360 *tps1-2 GVG::TPS1* when compared to *tps1-2 GVG::TPS1* (Fig. S4), such a role would likely
361 be indirect.

362 Understanding the interplay between energy metabolism, in particular *SnRK1*, TOR, and T6P
363 signaling, and plant growth and development is of utmost importance for developing plants
364 capable of withstanding future challenges. The suppressor mutants generated in the *tps1-2*
365 *GVG::TPS1* background comprise an important resource in our hunt for additional factors
366 that, like *HUA2*, link energy metabolism to plant development.

367

368 **Material and methods**

369 **Plant materials and growth conditions**

370 All T-DNA insertion mutants and transgenic lines used in this work are in the Col-0
371 background. The *tps1-2 GVG::TPS1* line used in this work is referred to as ind-TPS1 #201 in
372 the original publication (Dijken et al., 2004). The *hua2-4* (SALK_032281C) was obtained
373 from NASC and the presence of the T-DNA insertion was confirmed by PCR (Table S5).
374 *ft-10* (GABI-Kat: 290E08) was provided by Dr. Yi Zhang, Southern University of Science
375 and Technology, *flc-3* (Kim et al., 2006) by Dr. Liangyu Liu, Capital Normal University, and
376 *soc1-2* (Lee et al., 2000) by Dr. Jie Luo, Chinese Academy of Sciences. *tps1-2 GVG::TPS1*
377 *hua2-4* plants were generated by crossing and double homozygous mutants were identified by
378 phenotyping and genotyping of F2 individuals. Higher order mutants were obtained by
379 crossing *soc1-2*, *flc-3*, and *ft-10* mutants with the *tps1-2 GVG::TPS1 hua2-4* double mutant
380 and homozygous triple mutants were identified in the F2 and F3 generation. All mutant
381 genotypes were confirmed by PCR, see Table S7 for details. Plants were planted onto nutrient
382 soil with normal water supply and grown under either long days (LD) with a photoperiod of
383 16 hours light at 22°C and 8 hours darkness at 20°C or in short days (SD) with a photoperiod
384 of 8 hours light at 22°C and 16 hours darkness at 20°C. Flowering time are presented as
385 average rosette leaf number, cauline leaf number, and total leaf number.

386 **Genome sequencing and analysis**

387 Young leaves were used for DNA extraction for sequencing using the NovaSeq 6000
388 Sequencing platform (Novogene). Adapters and low-quality sequences of raw reads were
389 trimmed using Trimmomatic (Bolger et al., 2014), and the clean reads were mapped to the
390 reference genome of Col-0 using BWA-MEM (v0.7.15) (Cingolani et al., 2012). SNP calling
391 was performed using Genome Analysis Toolkit 4 (GATK4;
392 <https://gatk.broadinstitute.org/hc/en-us>) with default parameters. Variants were annotated
393 using snpEff 4.3 (Li and Durbin, 2009) based on TAIR 10 annotation. Next, we identified the
394 protein-coding genes with multiple non-redundant mutations and found three mutant lines

395 harboring unique non-synonymous mutations in the *HUA2* gene. The method was inspired by
396 our previous study that multiple EMS-induced mutants with unique mutation sites in the
397 coding regions of *SnRK1* alpha subunit rescued the non-flowering phenotype of *tps1*
398 (Zacharaki et al., 2022).

399 **Gene expression analysis by RNA-seq**

400 For RNA-seq analyses, plants were grown on soil for 3 weeks in LD conditions. Leaves from
401 21-day-old *Arabidopsis thaliana* were collected, immediately snap-frozen and stored at
402 -80°C . Total RNA was extracted using RNAprep Pure Plant Plus Kit (Tiangen, China,
403 DP441). RNA integrity was assessed using the RNA Nano 6000 Assay Kit on the
404 Bioanalyzer 2100 system (Agilent Technologies, CA, USA). RNA-seq libraries were
405 generated with three independent biological replicates and sequenced on the Illumina
406 NovaSeq platform by Annoroad Gene Technology. The raw RNA-seq reads were quality
407 trimmed by Trimmomatic (v 0.11.9) (Bolger et al., 2014). The qualified reads were mapped
408 to TAIR10 version genome guided by gene annotation model using HISAT2 (v2.1.0) (Kim et
409 al., 2015). The expression level for each gene was determined by StringTie (v1.3.4) (Pertea et
410 al., 2016). The differential expressed genes were identified by DESeq2 (Love et al., 2014).

411 **RNA isolation and RT-qPCR data analysis**

412 Total RNA was extracted from *Arabidopsis* seedlings using the RNA Isolation Kit (Tiangen,
413 China, DP441) according to the manufacturer's instructions. cDNA was synthesized from 3
414 μg total RNA in a 10 μl reaction volume using the RevertAid Premium First Strand cDNA
415 Synthesis Kit (Fermentas, Thermo Fisher Scientific, Rochester, NY). Quantitative real-time
416 PCR (qRT-PCR) was performed using TB GreenTM Premix Ex TaqTM II (Takara, Dalian,
417 China). Relative gene expression was calculated using the $2^{-\Delta\Delta\text{Ct}}$ method (Rao et al., 2013).
418 All analyses were repeated three times. The primer used for qRT-PCR are listed in
419 Supplemental Tables S5.

420 **Accession numbers**

421 Identifiers of key genes used in this study: *TPS1* (At1g78580), *HUA2* (AT5G23150), *SOCI*
422 (AT2G45660), *FLC* (AT5G10140), *FT* (AT1G65480). RNA-seq data generated in this study
423 have been deposited with NCBI under the BioProject PRJNA1005425.

424 **Data availability**

425 The data and material that support the findings of this study are available from the
426 corresponding author upon reasonable request.

427 **Author contributions**

428 LZ and MS designed the experiments. LZ carried out the SNP detection and genetic analyses
429 with input from VZ and MS. LZ carried out the gene expression analyses. LP and MS wrote
430 the manuscript with contributions from all authors.

431 **Acknowledgments**

432 The authors would like to thank Ruben M. Benstein and Vanessa Wahl for discussion and
433 comments on the manuscript. This work was supported by grants from the National Natural
434 Science Foundation of China (32071504 and 32371577) YW, the fundamental research funds
435 for the central universities (BLX202170) to LZ, and the DFG (SPP1530: SCHM1560/8-1, 8-2)
436 and the Swedish Research Council (2015-04617) to MS.

437 **References**

438 **Abe M, Kobayashi Y, Yamamoto S, Daimon Y, Yamaguchi A, Ikeda Y, Ichinoki H,**
439 **Notaguchi M, Goto K, Araki T** (2005) FD, a bZIP protein mediating signals from
440 the floral pathway integrator FT at the shoot apex. *Science* **309**: 1052-1056

441 **Baena-González E, Hanson J** (2017) Shaping plant development through the SnRK1-TOR
442 metabolic regulators. *Curr Opin Plant Biol* **35**: 152-157

443 **Baena-González E, Lunn JE** (2020) SnRK1 and trehalose 6-phosphate - two ancient
444 pathways converge to regulate plant metabolism and growth. *Curr Opin Plant Biol* **55**:
445 52-59

446 **Belda-Palazón B, Costa M, Beeckman T, Rolland F, Baena-González E** (2022) ABA
447 represses TOR and root meristem activity through nuclear exit of the SnRK1 kinase.
448 *Proc Natl Acad Sci USA* **119**: 1-3

449 **Blázquez MA, Santos E, Flores CL, Martínez-Zapater JM, Salinas J, Gancedo C** (1998)
450 Isolation and molecular characterization of the *Arabidopsis* TPS1 gene, encoding
451 trehalose-6-phosphate synthase. *Plant J* **13**: 685-689

452 **Blázquez MA, Weigel D** (2000) Integration of floral inductive signals in *Arabidopsis*. *Nature*
453 **404**: 889-892

454 **Bolger AM, Lohse M, Usadel B** (2014) Trimmomatic: a flexible trimmer for Illumina
455 sequence data. *Bioinformatics* **30**: 2114-2120

456 **Broucke E, Dang TTV, Li Y, Hulsmans S, Van Leene J, De Jaeger G, Hwang I, Wim**
457 **VdE, Rolland F** (2023) SnRK1 inhibits anthocyanin biosynthesis through both
458 transcriptional regulation and direct phosphorylation and dissociation of the
459 MYB/bHLH/TTG1 MBW complex. *Plant J* **115**: 1193-1213

460 **Cabib E, Leloir LF** (1958) THE BIOSYNTHESIS OF TREHALOSE PHOSPHATE. *Journal*
461 *of Biological Chemistry* **231**: 259-275

462 **Chary SN, Hicks GR, Choi YG, Carter D, Raikhel NV** (2008) Trehalose-6-phosphate
463 synthase/phosphatase regulates cell shape and plant architecture in *Arabidopsis*. *Plant*
464 *Physiol* **146**: 97-107

465 **Chen X, Meyerowitz EM** (1999) HUA1 and HUA2 are two members of the floral homeotic
466 AGAMOUS pathway. *Mol Cell* **3**: 349-360

467 **Cheng Y, Kato N, Wang W, Li J, Chen X** (2003) Two RNA binding proteins, HEN4 and
468 HUA1, act in the processing of AGAMOUS pre-mRNA in *Arabidopsis thaliana*. *Dev*
469 *Cell* **4**: 53-66

470 **Cho LH, Yoon J, An G** (2017) The control of flowering time by environmental factors. *Plant*
471 *J* **90**: 708-719

472 **Cingolani P, Platts A, Wang le L, Coon M, Nguyen T, Wang L, Land SJ, Lu X, Ruden**
473 **DM** (2012) A program for annotating and predicting the effects of single nucleotide
474 polymorphisms, SnpEff: SNPs in the genome of *Drosophila melanogaster* strain
475 w1118; iso-2; iso-3. *Fly (Austin)* **6**: 80-92

476 **Collani S, Neumann M, Yant L, Schmid M** (2019) FT Modulates Genome-Wide
477 DNA-Binding of the bZIP Transcription Factor FD. *Plant Physiol* **180**: 367-380

478 **Colombo M, Masiero S, Vanzulli S, Lardelli P, Kater MM, Colombo L** (2008) AGL23, a
479 type I MADS-box gene that controls female gametophyte and embryo development in

480 Arabidopsis. *Plant J* **54**: 1037-1048

481 **Corbesier L, Lejeune P, Bernier G** (1998) The role of carbohydrates in the induction of
482 flowering in *Arabidopsis thaliana*: comparison between the wild type and a starchless
483 mutant. *Planta* **206**: 131-137

484 **Delatte TL, Sedjani P, Kondou Y, Matsui M, de Jong GJ, Somsen GW, Wiese-Klinkenberg A, Primavesi LF, Paul MJ, Schluemann H** (2011) Growth
485 arrest by trehalose-6-phosphate: an astonishing case of primary metabolite control
486 over growth by way of the SnRK1 signaling pathway. *Plant Physiol* **157**: 160-174

487 **Delorge I, Figueroa CM, Feil R, Lunn JE, Van Dijck P** (2015) Trehalose-6-phosphate
488 synthase 1 is not the only active TPS in *Arabidopsis thaliana*. *Biochem J* **466**:
489 283-290

490 **Deng W, Ying H, Helliwell CA, Taylor JM, Peacock WJ, Dennis ES** (2011) FLOWERING
491 LOCUS C (FLC) regulates development pathways throughout the life cycle of
492 *Arabidopsis*. *Proc Natl Acad Sci USA* **108**: 6680-6685

493 **Dietrich K, Weltmeier F, Ehlert A, Weiste C, Stahl M, Harter K, Dröge-Laser W** (2011)
494 Heterodimers of the *Arabidopsis* transcription factors bZIP1 and bZIP53 reprogram
495 amino acid metabolism during low energy stress. *Plant Cell* **23**: 381-395

496 **Doyle MR, Bizzell CM, Keller MR, Michaels SD, Song J, Noh YS, Amasino RM** (2005)
497 HUA2 is required for the expression of floral repressors in *Arabidopsis thaliana*. *Plant*
498 *J* **41**: 376-385

499 **Eastmond PJ, van Dijken AJ, Spielman M, Kerr A, Tissier AF, Dickinson HG, Jones JD, Smeekens SC, Graham IA** (2002) Trehalose-6-phosphate synthase 1, which
500 catalyses the first step in trehalose synthesis, is essential for *Arabidopsis* embryo
501 maturation. *Plant J* **29**: 225-235

502 **Figueroa CM, Lunn JE** (2016) A Tale of Two Sugars: Trehalose 6-Phosphate and Sucrose.
503 *Plant Physiol* **172**: 7-27

504 **Gibson SI** (2005) Control of plant development and gene expression by sugar signaling. *Curr*
505 *Opin Plant Biol* **8**: 93-102

506 **Goddijn OJ, van Dun K** (1999) Trehalose metabolism in plants. *Trends Plant Sci* **4**:
507 315-319

508 **Ilk N, Ding J, Ihnatowicz A, Koornneef M, Reymond M** (2014) Natural variation for
509 anthocyanin accumulation under high-light and low-temperature stress is attributable
510 to the ENHANCER OF AG-4 2 (HUA2) locus in combination with PRODUCTION
511 OF ANTHOCYANIN PIGMENT1 (PAP1) and PAP2. *New Phytol* **206**: 422-435

512 **Jali SS, Rosloski SM, Janakirama P, Steffen JG, Zhurov V, Berleth T, Clark RM, Grbic V** (2014) A plant-specific HUA2-LIKE (HULK) gene family in *Arabidopsis thaliana*
513 is essential for development. *Plant J* **80**: 242-254

514 **Jung JH, Ju Y, Seo PJ, Lee JH, Park CM** (2012) The SOC1-SPL module integrates
515 photoperiod and gibberellic acid signals to control flowering time in *Arabidopsis*.
516 *Plant J* **69**: 577-588

517 **Kardailsky I, Shukla VK, Ahn JH, Dagenais N, Christensen SK, Nguyen JT, Chory J, Harrison MJ, Weigel D** (1999) Activation tagging of the floral inducer FT. *Science*
518 **286**: 1962-1965

519 **Kim D, Langmead B, Salzberg SL** (2015) HISAT: a fast spliced aligner with low memory

524 requirements. *Nat Methods* **12**: 357-360

525 **Kobayashi Y, Kaya H, Goto K, Iwabuchi M, Araki T** (1999) A pair of related genes with
526 antagonistic roles in mediating flowering signals. *Science* **286**: 1960-1962

527 **Kobayashi Y, Weigel D** (2007) Move on up, it's time for change--mobile signals controlling
528 photoperiod-dependent flowering. *Genes Dev* **21**: 2371-2384

529 **Koo SC, Bracko O, Park MS, Schwab R, Chun HJ, Park KM, Seo JS, Grbic V,**
530 **Balasubramanian S, Schmid M, Godard F, Yun DJ, Lee SY, Cho MJ, Weigel D,**
531 **Kim MC** (2010) Control of lateral organ development and flowering time by the
532 *Arabidopsis thaliana* MADS-box Gene AGAMOUS-LIKE6. *Plant J* **62**: 807-816

533 **Lee J, Lee I** (2010) Regulation and function of SOC1, a flowering pathway integrator. *J Exp*
534 *Bot* **61**: 2247-2254

535 **Lee JH, Ryu HS, Chung KS, Posé D, Kim S, Schmid M, Ahn JH** (2013) Regulation of
536 temperature-responsive flowering by MADS-box transcription factor repressors.
537 *Science* **342**: 628-632

538 **Lemus T, Mason GA, Bubb KL, Alexandre CM, Queitsch C, Cuperus JT** (2023) AGO1
539 and HSP90 buffer different genetic variants in *Arabidopsis thaliana*. *Genetics* **223**:
540 iyac163

541 **Leyman B, Van Dijck P, Thevelein JM** (2001) An unexpected plethora of trehalose
542 biosynthesis genes in *Arabidopsis thaliana*. *Trends Plant Sci* **6**: 510-513

543 **Li H, Durbin R** (2009) Fast and accurate short read alignment with Burrows-Wheeler
544 transform. *Bioinformatics* **25**: 1754-1760

545 **Li Y, Van den Ende W, Rolland F** (2014) Sucrose induction of anthocyanin biosynthesis is
546 mediated by DELLA. *Mol Plant* **7**: 570-572

547 **Liljegren SJ, Gustafson-Brown C, Pinyopich A, Ditta GS, Yanofsky MF** (1999)
548 Interactions among APETALA1, LEAFY, and TERMINAL FLOWER1 specify
549 meristem fate. *Plant Cell* **11**: 1007-1018

550 **Love MI, Huber W, Anders S** (2014) Moderated estimation of fold change and dispersion
551 for RNA-seq data with DESeq2. *Genome Biology* **15**: 1-21

552 **Lunn JE** (2007) Gene families and evolution of trehalose metabolism in plants. *Funct Plant*
553 *Biol* **34**: 550-563

554 **Lunn JE, Feil R, Hendriks JH, Gibon Y, Morcuende R, Osuna D, Scheible WR, Carillo**
555 **P, Hajirezaei MR, Stitt M** (2006) Sugar-induced increases in trehalose 6-phosphate
556 are correlated with redox activation of ADPglucose pyrophosphorylase and higher
557 rates of starch synthesis in *Arabidopsis thaliana*. *Biochem J* **397**: 139-148

558 **Mair A, Pedrotti L, Wurzinger B, Anrather D, Simeunovic A, Weiste C, Valerio C,**
559 **Dietrich K, Kirchler T, Naegele T, Vicente Carbajosa J, Hanson J,**
560 **Baena-Gonzalez E, Chaban C, Weckwerth W, Droege-Laser W, Teige M** (2015)
561 SnRK1-triggered switch of bZIP63 dimerization mediates the low-energy response in
562 plants. *Elife* **4**: 1-33

563 **Martins MC, Hejazi M, Fettke J, Steup M, Feil R, Krause U, Arrivault S, Vosloh D,**
564 **Figuerola CM, Ivakov A, Yadav UP, Piques M, Metzner D, Stitt M, Lunn JE**
565 (2013) Feedback inhibition of starch degradation in *Arabidopsis* leaves mediated by
566 trehalose 6-phosphate. *Plant Physiol* **163**: 1142-1163

567 **Mathieu J, Warthmann N, Kuttner F, Schmid M** (2007) Export of FT protein from phloem

568 companion cells is sufficient for floral induction in *Arabidopsis*. *Curr Biol* **17**:
569 1055-1060

570 **Meng LS, Xu MK, Wan W, Yu F, Li C, Wang JY, Wei ZQ, Lv MJ, Cao XY, Li ZY, Jiang**
571 **JH** (2018) Sucrose signaling regulates anthocyanin biosynthesis through a MAPK
572 cascade in *Arabidopsis thaliana*. *Genetics* **210**: 607-619

573 **Moon J, Lee H, Kim M, Lee I** (2005) Analysis of flowering pathway integrators in
574 *Arabidopsis*. *Plant Cell Physiol* **46**: 292-299

575 **Pertea M, Kim D, Pertea GM, Leek JT, Salzberg SL** (2016) Transcript-level expression
576 analysis of RNA-seq experiments with HISAT, StringTie and Ballgown. *Nat Protoc* **11**:
577 1650-1667

578 **Portereiko MF, Lloyd A, Steffen JG, Punwani JA, Otsuga D, Drews GN** (2006) AGL80 is
579 required for central cell and endosperm development in *Arabidopsis*. *Plant Cell* **18**:
580 1862-1872

581 **Posé D, Verhage L, Ott F, Yant L, Mathieu J, Angenent GC, Immink RG, Schmid M**
582 (2013) Temperature-dependent regulation of flowering by antagonistic FLM variants.
583 *Nature* **503**: 414-417

584 **Ramon M, De Smet I, Vandesteene L, Naudts M, Leyman B, Van Dijck P, Rolland F,**
585 **Beeckman T, Thevelein JM** (2009) Extensive expression regulation and lack of
586 heterologous enzymatic activity of the Class II trehalose metabolism proteins from
587 *Arabidopsis thaliana*. *Plant Cell Environ* **32**: 1015-1032

588 **Romera-Branchat M, Andrés F, Coupland G** (2014) Flowering responses to seasonal cues:
589 what's new? *Curr Opin Plant Biol* **21**: 120-127

590 **Singh V, Louis J, Ayre BG, Reese JC, Pegadaraju V, Shah J** (2011) TREHALOSE
591 PHOSPHATE SYNTHASE11-dependent trehalose metabolism promotes *Arabidopsis*
592 *thaliana* defense against the phloem-feeding insect *Myzus persicae*. *Plant J* **67**: 94-104

593 **Srikanth A, Schmid M** (2011) Regulation of flowering time: all roads lead to Rome. *Cell*
594 *Mol Life Sci* **68**: 2013-2037

595 **Taoka K, Ohki I, Tsuji H, Furuita K, Hayashi K, Yanase T, Yamaguchi M, Nakashima C,**
596 **Purwestri YA, Tamaki S, Ogaki Y, Shimada C, Nakagawa A, Kojima C,**
597 **Shimamoto K** (2011) 14-3-3 proteins act as intracellular receptors for rice Hd3a
598 florigen. *Nature* **476**: 332-335

599 **The 1001 Genomes Consortium** (2016) 1,135 genomes reveal the global pattern of
600 polymorphism in *Arabidopsis thaliana*. *Cell* **166**: 481-491.

601 **Tian L, Xie Z, Lu C, Hao X, Wu S, Huang Y, Li D, Chen L** (2019) The
602 trehalose-6-phosphate synthase TPS5 negatively regulates ABA signaling in
603 *Arabidopsis thaliana*. *Plant Cell Rep* **38**: 869-882

604 **Turck F, Fornara F, Coupland G** (2008) Regulation and identity of florigen: FLOWERING
605 LOCUS T moves center stage. *Annu Rev Plant Biol* **59**: 573-594

606 **Van Dijck P, Mascorro-Gallardo JO, De Bus M, Royackers K, Iturriaga G, Thevelein**
607 **JM** (2002) Truncation of *Arabidopsis thaliana* and *Selaginella lepidophylla*
608 trehalose-6-phosphate synthase unlocks high catalytic activity and supports high
609 trehalose levels on expression in yeast. *Biochem J* **366**: 63-71

610 **van Dijken AJ, Schluempf H, Smeekens SC** (2004) *Arabidopsis* trehalose-6-phosphate
611 synthase 1 is essential for normal vegetative growth and transition to flowering. *Plant*

612 Physiol 135: 969-977
613 **Van Leene J, Eeckhout D, Gadeyne A, Matthijs C, Han C, De Winne N, Persiau G, Van**
614 **De Slijke E, Persyn F, Mertens T, Smagghe W, Crepin N, Broucke E, Van**
615 **Damme D, Pleskot R, Rolland F, De Jaeger G** (2022) Mapping of the plant SnRK1
616 kinase signalling network reveals a key regulatory role for the class II T6P
617 synthase-like proteins. Nat Plants 8: 1245-1261
618 **Vandesteele L, López-Galvis L, Vanneste K, Feil R, Maere S, Lammens W, Rolland F,**
619 **Lunn JE, Avonce N, Beeckman T, Van Dijck P** (2012) Expansive evolution of the
620 trehalose-6-phosphate phosphatase gene family in Arabidopsis. Plant Physiol 160:
621 884-896
622 **Wahl V, Ponnu J, Schlereth A, Arrivault S, Langenecker T, Franke A, Feil R, Lunn JE,**
623 **Stitt M, Schmid M** (2013) Regulation of flowering by trehalose-6-phosphate
624 signaling in Arabidopsis thaliana. Science 339: 704-707
625 **Wang M, Zang L, Jiao F, Perez-Garcia M-D, Ogé L, Hamama L, Le Gourrierec J, Sakr**
626 **S, Chen J** (2020) Sugar Signaling and Post-transcriptional Regulation in Plants: An
627 Overlooked or an Emerging Topic? Front Plant Sci 11: 578096
628 **Wang Q, Sajja U, Rosloski S, Humphrey T, Kim MC, Bomblies K, Weigel D, Grbic V**
629 (2007) HUA2 caused natural variation in shoot morphology of *A. thaliana*. Curr Biol
630 17: 1513-1519
631 **Weigel D, Nilsson O** (1995) A developmental switch sufficient for flower initiation in diverse
632 plants. Nature 377: 495-500
633 **Wigge PA, Kim MC, Jaeger KE, Busch W, Schmid M, Lohmann JU, Weigel D** (2005)
634 Integration of spatial and temporal information during floral induction in Arabidopsis.
635 Science 309: 1056-1059
636 **Xing LB, Zhang D, Li YM, Shen YW, Zhao CP, Ma JJ, An N, Han MY** (2015)
637 Transcription Profiles Reveal Sugar and Hormone Signaling Pathways Mediating
638 Flower Induction in Apple (*Malus domestica* Borkh.). Plant Cell Physiol 56:
639 2052-2068
640 **Yadav UP, Ivakov A, Feil R, Duan GY, Walther D, Giavalisco P, Piques M, Carillo P,**
641 **Hubberten HM, Stitt M, Lunn JE** (2014) The sucrose-trehalose 6-phosphate (Tre6P)
642 nexus: specificity and mechanisms of sucrose signalling by Tre6P. J Exp Bot 65:
643 1051-1068
644 **Yan W, Chen D, Kaufmann K** (2016) Molecular mechanisms of floral organ specification
645 by MADS domain proteins. Curr Opin Plant Biol 29: 154-162
646 **Yoo SK, Chung KS, Kim J, Lee JH, Hong SM, Yoo SJ, Yoo SY, Lee JS, Ahn JH** (2005)
647 CONSTANS activates SUPPRESSOR OF OVEREXPRESSION OF CONSTANS 1
648 through FLOWERING LOCUS T to promote flowering in Arabidopsis. Plant Physiol
649 139: 770-778
650 **Zacharaki V, Ponnu J, Crepin N, Langenecker T, Hagmann J, Skorzinski N,**
651 **Musialak-Lange M, Wahl V, Rolland F, Schmid M** (2022) Impaired KIN10
652 function restores developmental defects in the Arabidopsis trehalose 6-phosphate
653 synthase1 (tps1) mutant. New Phytol 235: 220-233

654 **Figure legends**

655 **Figure 1. EMS-induced mutations in *HUA2* induce flowering in *tps1-2 GVG::TPS1***
656 **background. A)** Schematic drawing of *HUA2* indicating the position and the amino acid
657 changes caused by the EMS-induced mutations *hua2-11* (P455S), *hua2-12* (R902C), and
658 *hua2-13* (A983T). **B)** Phenotype of 9-week-old *tps1-2 GVG::TPS1*, *hua2-11 tps1-2*
659 *GVG::TPS1*, *hua2-12 tps1-2 GVG::TPS1*, *hua2-13 tps1-2 GVG::TPS1* and wild-type Col-0
660 *plants* grown in LD at 23°C. **C)** Flowering time of genotypes is given as total leaf number
661 (rosette (grey); cauline leaves (white)) determined after bolting. Error bars represent the
662 standard deviation. ANOVA Tukey's multiple comparisons test was applied, and letters
663 represent the statistical differences among genotypes ($P < 0.001$).

664

665 **Figure 2. A T-DNA insertion in *HUA2* partially rescues the flowering time phenotype of**
666 ***tps1-2 GVG::TPS1*. A)** Schematic drawing of the *HUA2* locus indicating the position of the
667 T-DNA insertion (SALK_032281C) in the 2nd intron in *hua2-4*. **B-C)** Phenotypic analysis (B)
668 and flowering time(C) of 9-week-old wild-type Col-0, *tps1-2 GVG::TPS1*, *hua2-4 tps1-2*
669 *GVG::TPS1* and *hua2-4* plants grown in LD at 23°C. Flowering time was scored as total leaf
670 number (rosette (grey) and cauline leaves (white)) after bolting. Error bars represent the
671 standard deviation. ANOVA Tukey's multiple comparisons test was applied, and letters
672 represent the statistical differences among genotypes ($P < 0.001$).

673

674 **Figure 3. Characterization of *hua2-4 tps1-2 GVG::TPS1* transcriptome. A)** 4-way Venn
675 diagram of genes that are differentially expressed in *tps1-2 GVG::TPS1* in response to
676 dexamethasone treatment and/or differentially expressed in *hua2-4 tps1-2 GVG::TPS1* when
677 compared to *tps1-2 GVG::TPS1*. **B)** GO analysis of 412 genes downregulated in *tps1-2*
678 *GVG::TPS1* in response to dexamethasone treatment and in *hua2-4 tps1-2 GVG::TPS1*. **C)**
679 GO analysis of 243 genes upregulated in *tps1-2 GVG::TPS1* in response to dexamethasone
680 treatment and in *hua2-4 tps1-2 GVG::TPS1*. **D)** Relative expression of *AGL24* and *SOC1* in
681 *tps1-2 GVG::TPS1* (white), *tps1-2 GVG::TPS1* treated with dexamethasone (black), and
682 *hua2-4 tps1-2 GVG::TPS1* (grey). *AGL24* and *SOC1* are significantly differentially expressed.

683 Error bars indicate the standard deviation. ANOVA Tukey's multiple comparisons test was
684 applied, and letters represent the statistical differences among genotypes ($P < 0.001$).

685

686 **Figure 4. Genetic interactions between *tps1-2*, *hua2-4*, and floral regulators *SOC1*, *FT*,
687 and *FLC*.** **A-B**) Phenotypes (**A**) and flowering time (**B**) of Col-0, *hua2-4*, *tps1-2* *GVG::TPS1*,
688 and *soc1-2* mutant combinations. **D-E**) Phenotypes (**D**) and flowering time (**E**) of Col-0,
689 *hua2-4*, *tps1-2* *GVG::TPS1*, and *ft-10* mutant combinations. **G-H**) Phenotypes (**G**) and
690 flowering time (**H**) of Col-0, *hua2-4*, *tps1-2* *GVG::TPS1*, and *flc-3* mutant combinations.
691 Flowering time (**B**, **E**, **H**) was scored as total leaf number (rosette (grey) and caulin leaves
692 (white)) after bolting. **C, F, I**) Relative expression of *SOC1* (**C**), *FT* (**F**), and *FLC* (**I**) in
693 *tps1-2* *GVG::TPS1* and *hua2-4* *tps1-2* *GVG::TPS1*. Gene expression was determined by
694 RT-qPCR at the end of the long day (ZT 16). Error bars represent the standard deviation.
695 ANOVA Tukey's multiple comparisons test was applied, and letters represent the statistical
696 differences among genotypes ($P < 0.001$).

697

698 **Figure 5. Loss of *FLC* rescues the non-flowering phenotype of *tps1-2* *GVG::TPS1*.** **A)**
699 VST expression estimates for MADS-box floral repressors in 18-day-old plants. RNA-seq
700 expression data retrieved from Zacharaki et al., 2022. Columns indicate mean VST
701 expression estimates as implemented in DEseq2 calculated from three individual biological
702 replicates per genotype. Circles indicate expression estimates for individual biological
703 replicates. Asterisks indicate differential gene expression with a statistical significance of
704 $P_{adj} < 0.01$. **B-C)** Phenotypes (**B**) and total leaf number (**C**) of Col-0, *tps1-2* *GVG::TPS1*,
705 *flc-3*, and *flc-3* *tps1-2* *GVG::TPS1* double mutant. Flowering time was scored as total leaf
706 number (rosette (grey) and caulin leaves (white)) after bolting. Error bars represent the
707 standard deviation. ANOVA Tukey's multiple comparisons test was applied, and letters
708 represent the statistical differences among genotypes ($P < 0.001$).

709

710 **Figure 6. Expression of SnRK1 target genes *SEN5* and *DIN6* in *hua2-4* and *hua2-4*
711 *tps1-2* *GVG::TPS1* double mutant.** **A-B)** Induction of *SEN5* (**A**) and *DIN6* (**B**) in response
712 to extended night is attenuated in 14-day-old of *hua2-4* single mutant and three independent

713 lines of the *hua2-4 tps1-2 GVG::TPS1* double mutant. Plants were grown for 14 days in LD
714 (grey) before being exposed to a single extended night (12h additional darkness; black). LD,
715 long days. Error bars represent the standard deviation. ANOVA Tukey's multiple comparisons
716 test was applied, and letters represent the statistical differences among genotypes ($P < 0.001$).

717 **Supplemental Material**

718 **Supplemental Figure S1** Relative expression of *HUA2* in *tps1-2 GVG::TPS1* treated
719 with dexamethasone or untreated.

720 **Supplemental Figure S2** Relative expression of important floral regulators in *tps1-2*
721 *GVG::TPS1*, *tps1-2 GVG::TPS1* treated with dexamethasone,
722 and *hua2-4 tps1-2 GVG::TPS1*.

723 **Supplemental Figure S3** VST expression estimates for *HUA2* in 18-day-old plants.

724 **Supplemental Figure S4** Relative expression of SnRK1 subunits in *tps1-2*
725 *GVG::TPS1*, *tps1-2 GVG::TPS1* treated with dexamethasone,
726 and *hua2-4 tps1-2 GVG::TPS1*.

727 **Supplemental Table S1** Number of SNPs identified in individual suppressor mutants.

728 **Supplemental Table S2** Number of SNPs identified in EMS suppressor lines carrying
729 mutations in *HUA2*.

730 **Supplemental Table S3** EMS suppressor lines bearing non-synonymous mutations in
731 *HUA2*.

732 **Supplemental Table S4** GO analysis of 412 genes downregulated in *tps1-2*
733 *GVG::TPS1* in response to dexamethasone application and in
734 *hua2-4*.

735 **Supplemental Table S5** GO analysis of 243 genes induced in *tps1-2 GVG::TPS1* in
736 response to dexamethasone application and in *hua2-4*.

737 **Supplemental Table S6** Expression of flowering time genes in *hua2-4 tps1-2*
738 *GVG::TPS1* and *tps1-2 GVG::TPS1*.

739 **Supplemental Table S7** List of oligonucleotides used in this study.

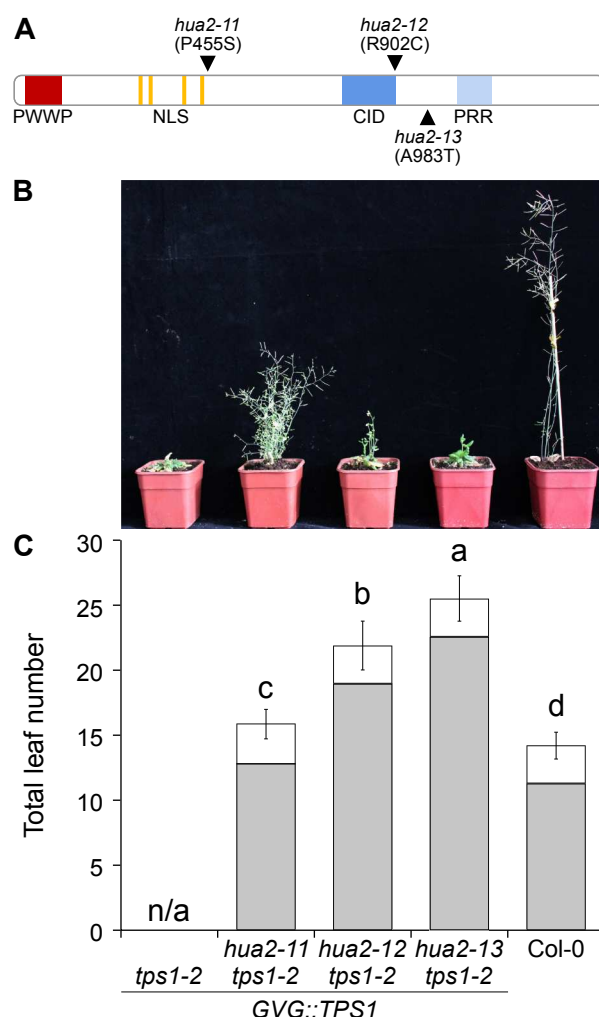


Figure 1. EMS-induced mutations in *HUA2* induce flowering in *tps1-2 GVG::TPS1* background. A) Schematic drawing of HUA2 indicating the position and the amino acid changes caused by the EMS-induced mutations *hua2-11* (P455S), *hua2-12* (R902C), and *hua2-13* (A983T). **B)** Phenotype of 9-week-old *tps1-2 GVG::TPS1*, *hua2-11 tps1-2 GVG::TPS1*, *hua2-12 tps1-2 GVG::TPS1*, *hua2-13 tps1-2 GVG::TPS1* and wild-type Col-0 plants grown in LD at 23°C. **C)** Flowering time of genotypes is given as total leaf number (rosette (grey); cauline leaves (white)) determined after bolting. Error bars represent the standard deviation. ANOVA Tukey's multiple comparisons test was applied, and letters represent the statistical differences among genotypes ($P < 0.001$).

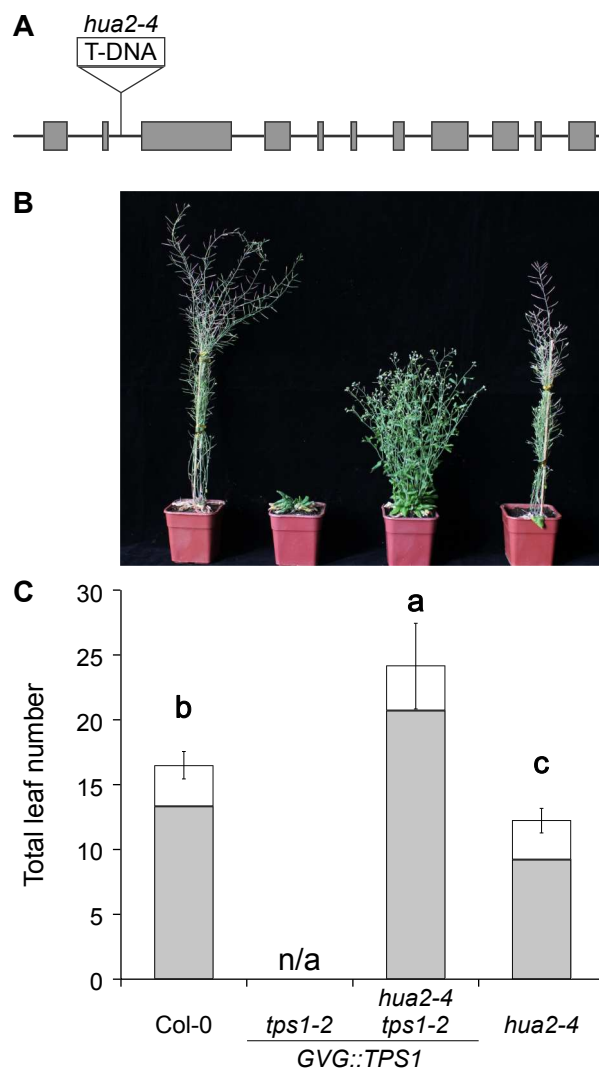


Figure 2. A T-DNA insertion in *HUA2* partially rescues the flowering time phenotype of *tps1-2 GVG::TPS1*. **A)** Schematic drawing of the *HUA2* locus indicating the position of the T-DNA insertion (SALK_032281C) in the 2nd intron in *hua2-4*. **B-C)** Phenotypic analysis (B) and flowering time(C) of 9-week-old wild-type Col-0, *tps1-2 GVG::TPS1*, *hua2-4 tps1-2 GVG::TPS1* and *hua2-4* plants grown in LD at 23°C. Flowering time was scored as total leaf number (rosette (grey) and cauline leaves (white)) after bolting. Error bars represent the standard deviation. ANOVA Tukey's multiple comparisons test was applied, and letters represent the statistical differences among genotypes ($P < 0.001$).

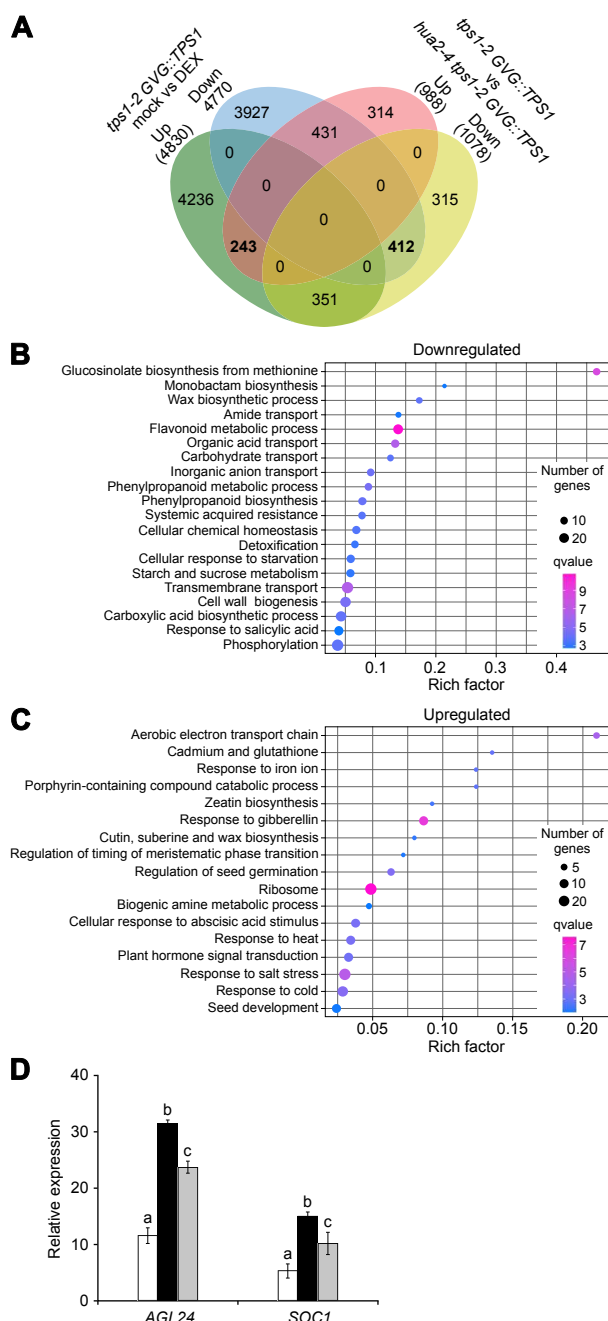


Figure 3. Characterization of *hua2-4 tps1-2 GVG::TPS1* transcriptome. A) 4-way Venn diagram of genes that are differentially expressed in *tpsl-2 GVG::TPS1* in response to dexamethasone treatment and/or differentially expressed in *hua2-4 tpsl-2 GVG::TPS1* when compared to *tpsl-2 GVG::TPS1*. **B)** GO analysis of 412 genes downregulated in *tpsl-2 GVG::TPS1* in response to dexamethasone treatment and in *hua2-4 tpsl-2 GVG::TPS1*. **C)** GO analysis of 243 genes upregulated in *tpsl-2 GVG::TPS1* in response to dexamethasone treatment and in *hua2-4 tpsl-2 GVG::TPS1*. **D)** Relative expression of *AGL24* and *SOC1* in *tpsl-2 GVG::TPS1* (white), *tpsl-2 GVG::TPS1* treated with dexamethasone (black), and *hua2-4 tpsl-2 GVG::TPS1* (grey). *AGL24* and *SOC1* are significantly differentially expressed. Error bars indicate the standard deviation. ANOVA Tukey's multiple comparisons test was applied, and letters represent the statistical differences among genotypes ($P < 0.001$).

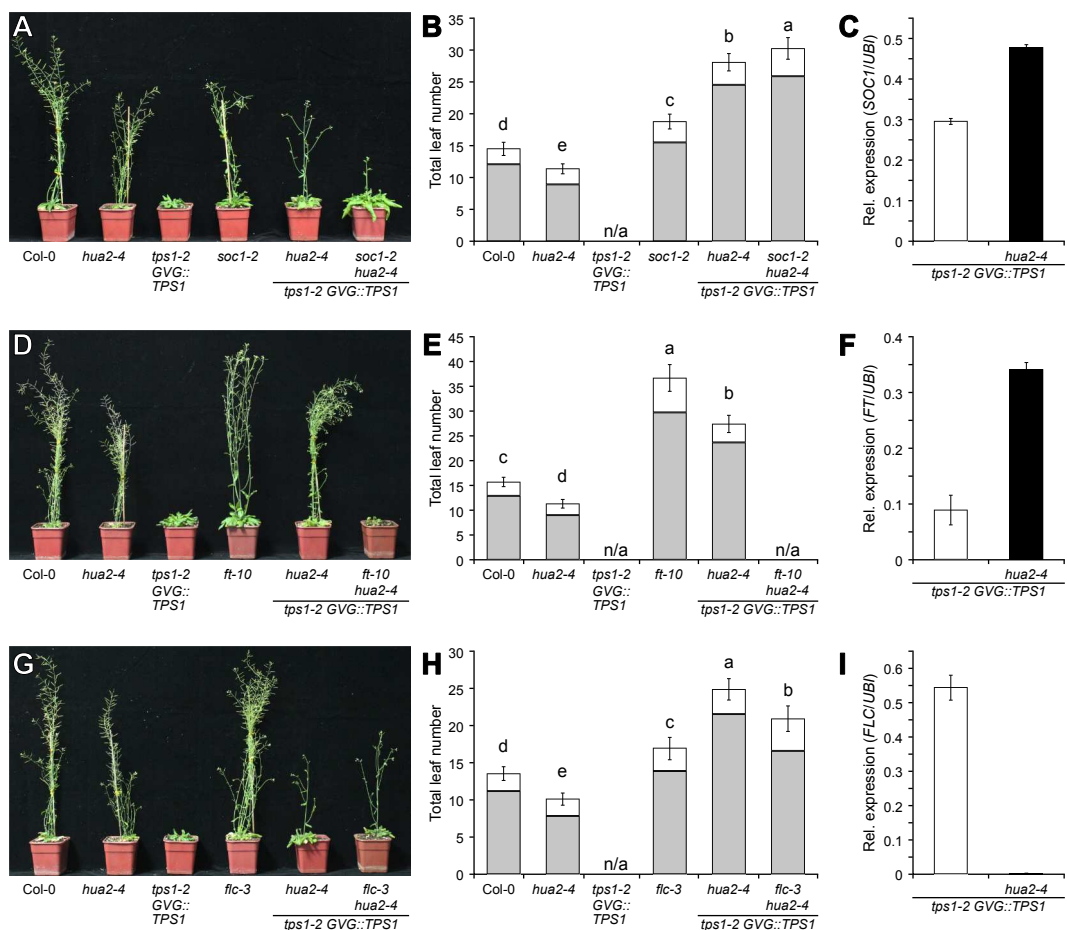


Figure 4. Genetic interactions between *tps1-2*, *hua2-4*, and floral regulators *SOC1*, *FT*, and *FLC*. **A-B)** Phenotypes (A) and flowering time (B) of Col-0, *hua2-4*, *tps1-2 GVG::TPS1*, and *soc1-2* mutant combinations. **D-E)** Phenotypes (D) and flowering time (E) of Col-0, *hua2-4*, *tps1-2 GVG::TPS1*, and *ft-10* mutant combinations. **G-H)** Phenotypes (G) and flowering time (H) of Col-0, *hua2-4*, *tps1-2 GVG::TPS1*, and *flc-3* mutant combinations. Flowering time (B, E, H) was scored as total leaf number (rosette (grey) and cauline leaves (white)) after bolting. **C, F, I)** Relative expression of *SOC1* (C), *FT* (F), and *FLC* (I) in *tps1-2 GVG::TPS1* and *hua2-4 tps1-2 GVG::TPS1*. Gene expression was determined by RT-qPCR at the end of the long day (ZT 16). Error bars represent the standard deviation. ANOVA Tukey's multiple comparisons test was applied, and letters represent the statistical differences among genotypes ($P < 0.001$).

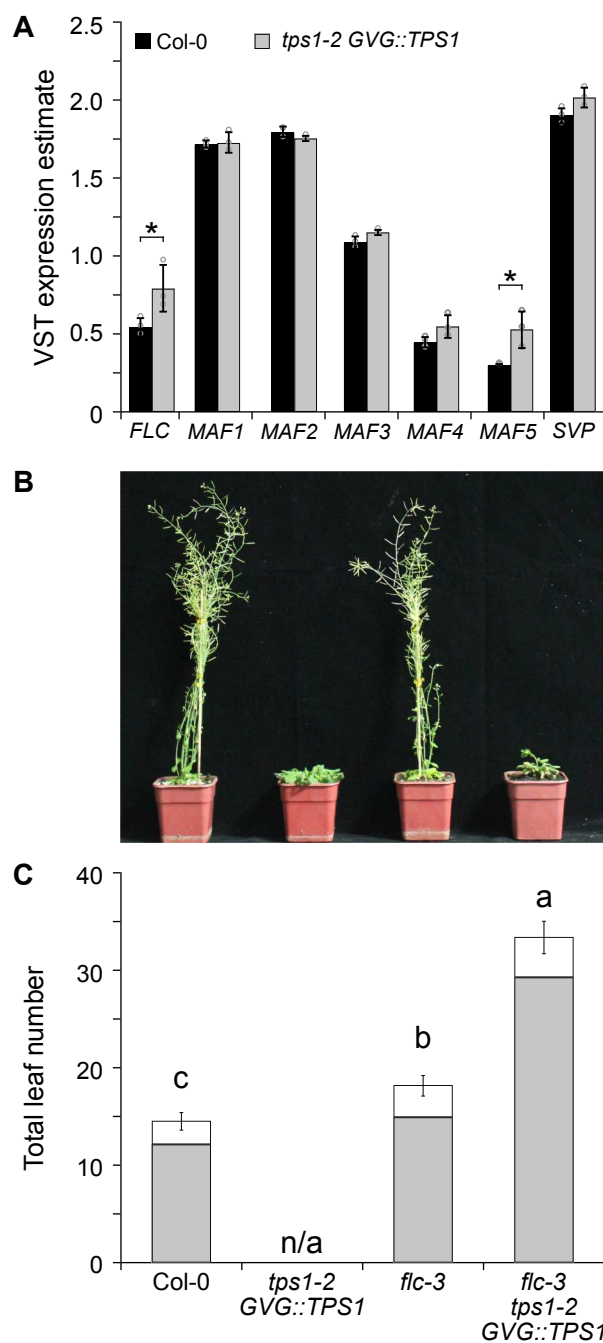


Figure 5. Loss of *FLC* rescues the non-flowering phenotype of *tps1-2 GVG::TPS1*. **A)** VST expression estimates for MADS-box floral repressors in 18-day-old plants. RNA-seq expression data retrieved from Zacharaki et al., 2022. Columns indicate mean VST expression estimates as implemented in DEseq2 calculated from three individual biological replicates per genotype. Circles indicate expression estimates for individual biological replicates. Asterisks indicate differential gene expression with a statistical significance of $P_{adj} < 0.01$. **B-C)** Phenotypes (**B**) and total leaf number (**C**) of Col-0, *tps1-2 GVG::TPS1*, *flc-3*, and *flc-3 tps1-2 GVG::TPS1 double mutant*. Flowering time was scored as total leaf number (rosette (grey) and cauline leaves (white)) after bolting. Error bars represent the standard deviation. ANOVA Tukey's multiple comparisons test was applied, and letters represent the statistical differences among genotypes ($P < 0.001$).

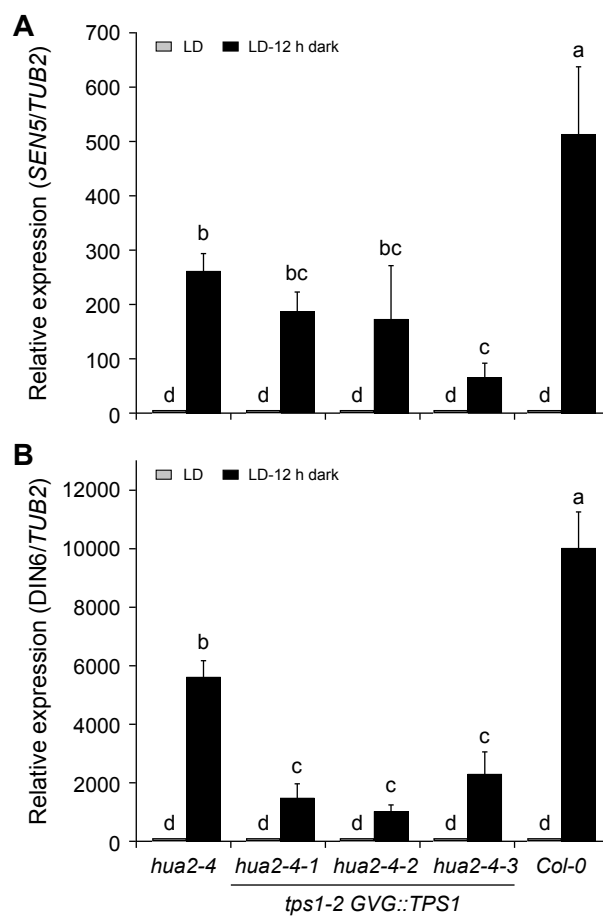


Figure 6. Expression of SnRK1 target genes *SEN5* and *DIN6* in *hua2-4* and *hua2-4 tps1-2 GVG::TPS1* double mutant. A-B) Induction of *SEN5* (A) and *DIN6* (B) in response to extended night is attenuated in 14-day-old of *hua2-4* single mutant and three independent lines of the *hua2-4 tps1-2 GVG::TPS1* double mutant. Plants were grown for 14 days in LD (grey) before being exposed to a single extended night (12h additional darkness; black). LD, long days. Error bars represent the standard deviation. ANOVA Tukey's multiple comparisons test was applied, and letters represent the statistical differences among genotypes ($P < 0.001$).

Parsed Citations

Abe M, Kobayashi Y, Yamamoto S, Daimon Y, Yamaguchi A, Ikeda Y, Ichinoki H, Notaguchi M, Goto K, Araki T (2005) FD, a bZIP protein mediating signals from the floral pathway integrator FT at the shoot apex. *Science* 309: 1052-1056

Google Scholar: [Author Only](#) [Title Only](#) [Author and Title](#)

Baena-González E, Hanson J (2017) Shaping plant development through the SnRK1-TOR metabolic regulators. *Curr Opin Plant Biol* 35: 152-157

Google Scholar: [Author Only](#) [Title Only](#) [Author and Title](#)

Baena-González E, Lunn JE (2020) SnRK1 and trehalose 6-phosphate - two ancient pathways converge to regulate plant metabolism and growth. *Curr Opin Plant Biol* 55: 52-59

Google Scholar: [Author Only](#) [Title Only](#) [Author and Title](#)

Belda-Palazón B, Costa M, Beeckman T, Rolland F, Baena-González E (2022) ABA represses TOR and root meristem activity through nuclear exit of the SnRK1 kinase. *Proc Natl Acad Sci USA* 119: 1-3

Google Scholar: [Author Only](#) [Title Only](#) [Author and Title](#)

Blázquez MA, Santos E, Flores CL, Martínez-Zapater JM, Salinas J, Gancedo C (1998) Isolation and molecular characterization of the *Arabidopsis* TPS1 gene, encoding trehalose-6-phosphate synthase. *Plant J* 13: 685-689

Google Scholar: [Author Only](#) [Title Only](#) [Author and Title](#)

Blázquez MA, Weigel D (2000) Integration of floral inductive signals in *Arabidopsis*. *Nature* 404: 889-892

Google Scholar: [Author Only](#) [Title Only](#) [Author and Title](#)

Bolger AM, Lohse M, Usadel B (2014) Trimmomatic: a flexible trimmer for Illumina sequence data. *Bioinformatics* 30: 2114-2120

Google Scholar: [Author Only](#) [Title Only](#) [Author and Title](#)

Broucke E, Dang TTV, Li Y, Hulsmans S, Van Leene J, De Jaeger G, Hwang I, Wim VdE, Rolland F (2023) SnRK1 inhibits anthocyanin biosynthesis through both transcriptional regulation and direct phosphorylation and dissociation of the MYB/bHLH/TTG1 MBW complex. *Plant J* 115: 1193-1213

Google Scholar: [Author Only](#) [Title Only](#) [Author and Title](#)

Cabib E, Leloir LF (1958) THE BIOSYNTHESIS OF TREHALOSE PHOSPHATE. *Journal of Biological Chemistry* 231: 259-275

Google Scholar: [Author Only](#) [Title Only](#) [Author and Title](#)

Chary SN, Hicks GR, Choi YG, Carter D, Raikhel NV (2008) Trehalose-6-phosphate synthase/phosphatase regulates cell shape and plant architecture in *Arabidopsis*. *Plant Physiol* 146: 97-107

Google Scholar: [Author Only](#) [Title Only](#) [Author and Title](#)

Chen X, Meyerowitz EM (1999) HUA1 and HUA2 are two members of the floral homeotic AGAMOUS pathway. *Mol Cell* 3: 349-360

Google Scholar: [Author Only](#) [Title Only](#) [Author and Title](#)

Cheng Y, Kato N, Wang W, Li J, Chen X (2003) Two RNA binding proteins, HEN4 and HUA1, act in the processing of AGAMOUS pre-mRNA in *Arabidopsis thaliana*. *Dev Cell* 4: 53-66

Google Scholar: [Author Only](#) [Title Only](#) [Author and Title](#)

Cho LH, Yoon J, An G (2017) The control of flowering time by environmental factors. *Plant J* 90: 708-719

Google Scholar: [Author Only](#) [Title Only](#) [Author and Title](#)

Cingolani P, Platts A, Wang le L, Coon M, Nguyen T, Wang L, Land SJ, Lu X, Ruden DM (2012) A program for annotating and predicting the effects of single nucleotide polymorphisms, SnpEff: SNPs in the genome of *Drosophila melanogaster* strain w1118; iso-2; iso-3. *Fly (Austin)* 6: 80-92

Google Scholar: [Author Only](#) [Title Only](#) [Author and Title](#)

Collani S, Neumann M, Yant L, Schmid M (2019) FT Modulates Genome-Wide DNA-Binding of the bZIP Transcription Factor FD. *Plant Physiol* 180: 367-380

Google Scholar: [Author Only](#) [Title Only](#) [Author and Title](#)

Colombo M, Masiero S, Vanzulli S, Lardelli P, Kater MM, Colombo L (2008) AGL23, a type I MADS-box gene that controls female gametophyte and embryo development in *Arabidopsis*. *Plant J* 54: 1037-1048

Google Scholar: [Author Only](#) [Title Only](#) [Author and Title](#)

Corbesier L, Lejeune P, Bernier G (1998) The role of carbohydrates in the induction of flowering in *Arabidopsis thaliana*: comparison between the wild type and a starchless mutant. *Planta* 206: 131-137

Google Scholar: [Author Only](#) [Title Only](#) [Author and Title](#)

Delatte TL, Sedjani P, Kondou Y, Matsui M, de Jong GJ, Somsen GW, Wiese-Klinkenberg A, Primavesi LF, Paul MJ, Schluemann H (2011) Growth arrest by trehalose-6-phosphate: an astonishing case of primary metabolite control over growth by way of the SnRK1 signaling pathway. *Plant Physiol* 157: 160-174

Google Scholar: [Author Only](#) [Title Only](#) [Author and Title](#)

Delorge I, Figueroa CM, Feil R, Lunn JE, Van Dijck P (2015) Trehalose-6-phosphate synthase 1 is not the only active TPS in *Arabidopsis thaliana*. *Biochem J* 466: 283-290

Google Scholar: [Author Only](#) [Title Only](#) [Author and Title](#)

Deng W, Ying H, Helliwell CA, Taylor JM, Peacock WJ, Dennis ES (2011) FLOWERING LOCUS C (FLC) regulates development pathways throughout the life cycle of *Arabidopsis*. *Proc Natl Acad Sci USA* 108: 6680-6685

Google Scholar: [Author Only](#) [Title Only](#) [Author and Title](#)

Dietrich K, Weltmeier F, Ehler A, Weiste C, Stahl M, Harter K, Dröge-Laser W (2011) Heterodimers of the *Arabidopsis* transcription factors bZIP1 and bZIP53 reprogram amino acid metabolism during low energy stress. *Plant Cell* 23: 381-395

Google Scholar: [Author Only](#) [Title Only](#) [Author and Title](#)

Doyle MR, Bizzell CM, Keller MR, Michaels SD, Song J, Noh YS, Amasino RM (2005) HUA2 is required for the expression of floral repressors in *Arabidopsis thaliana*. *Plant J* 41: 376-385

Google Scholar: [Author Only](#) [Title Only](#) [Author and Title](#)

Eastmond PJ, van Dijken AJ, Spielman M, Kerr A, Tissier AF, Dickinson HG, Jones JD, Smeekens SC, Graham IA (2002) Trehalose-6-phosphate synthase 1, which catalyses the first step in trehalose synthesis, is essential for *Arabidopsis* embryo maturation. *Plant J* 29: 225-235

Google Scholar: [Author Only](#) [Title Only](#) [Author and Title](#)

Figueroa CM, Lunn JE (2016) A Tale of Two Sugars: Trehalose 6-Phosphate and Sucrose. *Plant Physiol* 172: 7-27

Google Scholar: [Author Only](#) [Title Only](#) [Author and Title](#)

Gibson SI (2005) Control of plant development and gene expression by sugar signaling. *Curr Opin Plant Biol* 8: 93-102

Google Scholar: [Author Only](#) [Title Only](#) [Author and Title](#)

Goddijn OJ, van Dun K (1999) Trehalose metabolism in plants. *Trends Plant Sci* 4: 315-319

Google Scholar: [Author Only](#) [Title Only](#) [Author and Title](#)

Ilk N, Ding J, Ihnatowicz A, Koornneef M, Reymond M (2014) Natural variation for anthocyanin accumulation under high-light and low-temperature stress is attributable to the ENHANCER OF AG-4 2 (HUA2) locus in combination with PRODUCTION OF ANTHOCYANIN PIGMENT1 (PAP1) and PAP2. *New Phytol* 206: 422-435

Google Scholar: [Author Only](#) [Title Only](#) [Author and Title](#)

Jali SS, Rosłoski SM, Janakirama P, Steffen JG, Zhurov V, Berleth T, Clark RM, Grbic V (2014) A plant-specific HUA2-LIKE (HULK) gene family in *Arabidopsis thaliana* is essential for development. *Plant J* 80: 242-254

Google Scholar: [Author Only](#) [Title Only](#) [Author and Title](#)

Jung JH, Ju Y, Seo PJ, Lee JH, Park CM (2012) The SOC1-SPL module integrates photoperiod and gibberellin acid signals to control flowering time in *Arabidopsis*. *Plant J* 69: 577-588

Google Scholar: [Author Only](#) [Title Only](#) [Author and Title](#)

Kardailsky I, Shukla VK, Ahn JH, Dagenais N, Christensen SK, Nguyen JT, Chory J, Harrison MJ, Weigel D (1999) Activation tagging of the floral inducer FT. *Science* 286: 1962-1965

Google Scholar: [Author Only](#) [Title Only](#) [Author and Title](#)

Kim D, Langmead B, Salzberg SL (2015) HISAT: a fast spliced aligner with low memory requirements. *Nat Methods* 12: 357-360

Google Scholar: [Author Only](#) [Title Only](#) [Author and Title](#)

Kobayashi Y, Kaya H, Goto K, Iwabuchi M, Araki T (1999) A pair of related genes with antagonistic roles in mediating flowering signals. *Science* 286: 1960-1962

Google Scholar: [Author Only](#) [Title Only](#) [Author and Title](#)

Kobayashi Y, Weigel D (2007) Move on up, it's time for change--mobile signals controlling photoperiod-dependent flowering. *Genes Dev* 21: 2371-2384

Google Scholar: [Author Only](#) [Title Only](#) [Author and Title](#)

Koo SC, Bracko O, Park MS, Schwab R, Chun HJ, Park KM, Seo JS, Grbic V, Balasubramanian S, Schmid M, Godard F, Yun DJ, Lee SY, Cho MJ, Weigel D, Kim MC (2010) Control of lateral organ development and flowering time by the *Arabidopsis thaliana* MADS-box Gene AGAMOUS-LIKE6. *Plant J* 62: 807-816

Google Scholar: [Author Only](#) [Title Only](#) [Author and Title](#)

Lee J, Lee I (2010) Regulation and function of SOC1, a flowering pathway integrator. *J Exp Bot* 61: 2247-2254

Google Scholar: [Author Only](#) [Title Only](#) [Author and Title](#)

Lee JH, Ryu HS, Chung KS, Posé D, Kim S, Schmid M, Ahn JH (2013) Regulation of temperature-responsive flowering by MADS-box transcription factor repressors. *Science* 342: 628-632

Google Scholar: [Author Only](#) [Title Only](#) [Author and Title](#)

Lemus T, Mason GA, Bubb KL, Alexandre CM, Queitsch C, Cuperus JT (2023) AGO1 and HSP90 buffer different genetic variants in *Arabidopsis thaliana*. *Genetics* 223: iyac163

Google Scholar: [Author Only](#) [Title Only](#) [Author and Title](#)

Leyman B, Van Dijck P, Thevelein JM (2001) An unexpected plethora of trehalose biosynthesis genes in *Arabidopsis thaliana*. *Trends Plant Sci* 6: 510-513

Google Scholar: [Author Only](#) [Title Only](#) [Author and Title](#)

Li H, Durbin R (2009) Fast and accurate short read alignment with Burrows-Wheeler transform. *Bioinformatics* 25: 1754-1760

Google Scholar: [Author Only](#) [Title Only](#) [Author and Title](#)

Li Y, Van den Ende W, Rolland F (2014) Sucrose induction of anthocyanin biosynthesis is mediated by DELLA. *Mol Plant* 7: 570-572

Google Scholar: [Author Only](#) [Title Only](#) [Author and Title](#)

Liljegren SJ, Gustafson-Brown C, Pinyopich A, Ditta GS, Yanofsky MF (1999) Interactions among APETALA1, LEAFY, and TERMINAL FLOWER1 specify meristem fate. *Plant Cell* 11: 1007-1018

Google Scholar: [Author Only](#) [Title Only](#) [Author and Title](#)

Love MI, Huber W, Anders S (2014) Moderated estimation of fold change and dispersion for RNA-seq data with DESeq2. *Genome Biology* 15: 1-21

Google Scholar: [Author Only](#) [Title Only](#) [Author and Title](#)

Lunn JE (2007) Gene families and evolution of trehalose metabolism in plants. *Funct Plant Biol* 34: 550-563

Google Scholar: [Author Only](#) [Title Only](#) [Author and Title](#)

Lunn JE, Feil R, Hendriks JH, Gibon Y, Morcuende R, Osuna D, Scheible WR, Carillo P, Hajirezaei MR, Stitt M (2006) Sugar-induced increases in trehalose 6-phosphate are correlated with redox activation of ADPglucose pyrophosphorylase and higher rates of starch synthesis in *Arabidopsis thaliana*. *Biochem J* 397: 139-148

Google Scholar: [Author Only](#) [Title Only](#) [Author and Title](#)

Mair A, Pedrotti L, Wurzinger B, Anrather D, Simeunovic A, Weiste C, Valerio C, Dietrich K, Kirchler T, Naegele T, Vicente Carabajosa J, Hanson J, Baena-Gonzalez E, Chaban C, Weckwerth W, Droege-Laser W, Teige M (2015) SnRK1-triggered switch of bZIP63 dimerization mediates the low-energy response in plants. *Elife* 4: 1-33

Google Scholar: [Author Only](#) [Title Only](#) [Author and Title](#)

Martins MC, Hejazi M, Fettke J, Steup M, Feil R, Krause U, Arrivault S, Vosloh D, Figueroa CM, Ivakov A, Yadav UP, Piques M, Metzner D, Stitt M, Lunn JE (2013) Feedback inhibition of starch degradation in *Arabidopsis* leaves mediated by trehalose 6-phosphate. *Plant Physiol* 163: 1142-1163

Google Scholar: [Author Only](#) [Title Only](#) [Author and Title](#)

Mathieu J, Warthmann N, Kuttner F, Schmid M (2007) Export of FT protein from phloem companion cells is sufficient for floral induction in *Arabidopsis*. *Curr Biol* 17: 1055-1060

Google Scholar: [Author Only](#) [Title Only](#) [Author and Title](#)

Meng LS, Xu MK, Wan W, Yu F, Li C, Wang JY, Wei ZQ, Lv MJ, Cao XY, Li ZY, Jiang JH (2018) Sucrose signaling regulates anthocyanin biosynthesis through a MAPK cascade in *Arabidopsis thaliana*. *Genetics* 210: 607-619

Google Scholar: [Author Only](#) [Title Only](#) [Author and Title](#)

Moon J, Lee H, Kim M, Lee I (2005) Analysis of flowering pathway integrators in *Arabidopsis*. *Plant Cell Physiol* 46: 292-299

Google Scholar: [Author Only](#) [Title Only](#) [Author and Title](#)

Pertea M, Kim D, Pertea GM, Leek JT, Salzberg SL (2016) Transcript-level expression analysis of RNA-seq experiments with HISAT, StringTie and Ballgown. *Nat Protoc* 11: 1650-1667

Google Scholar: [Author Only](#) [Title Only](#) [Author and Title](#)

Portereiko MF, Lloyd A, Steffen JG, Punwani JA, Otsuga D, Drews GN (2006) AGL80 is required for central cell and endosperm development in *Arabidopsis*. *Plant Cell* 18: 1862-1872

Google Scholar: [Author Only](#) [Title Only](#) [Author and Title](#)

Posé D, Verhage L, Ott F, Yant L, Mathieu J, Angenent GC, Immink RG, Schmid M (2013) Temperature-dependent regulation of flowering by antagonistic FLM variants. *Nature* 503: 414-417

Google Scholar: [Author Only](#) [Title Only](#) [Author and Title](#)

Ramon M, De Smet I, Vandesteene L, Naudts M, Leyman B, Van Dijck P, Rolland F, Beeckman T, Thevelein JM (2009) Extensive expression regulation and lack of heterologous enzymatic activity of the Class II trehalose metabolism proteins from *Arabidopsis thaliana*. *Plant Cell Environ* 32: 1015-1032

Google Scholar: [Author Only](#) [Title Only](#) [Author and Title](#)

Romera-Branchat M, Andrés F, Coupland G (2014) Flowering responses to seasonal cues: what's new? *Curr Opin Plant Biol* 21: 120-127

Google Scholar: [Author Only](#) [Title Only](#) [Author and Title](#)

Singh V, Louis J, Ayre BG, Reese JC, Pegadaraju V, Shah J (2011) TREHALOSE PHOSPHATE SYNTHASE11-dependent trehalose metabolism promotes *Arabidopsis thaliana* defense against the phloem-feeding insect *Myzus persicae*. *Plant J* 67: 94-104

Google Scholar: [Author Only](#) [Title Only](#) [Author and Title](#)

Srikanth A, Schmid M (2011) Regulation of flowering time: all roads lead to Rome. *Cell Mol Life Sci* 68: 2013-2037

Google Scholar: [Author Only](#) [Title Only](#) [Author and Title](#)

Taoka K, Ohki I, Tsuji H, Furuita K, Hayashi K, Yanase T, Yamaguchi M, Nakashima C, Purwestri YA, Tamaki S, Ogaki Y, Shimada C, Nakagawa A, Kojima C, Shimamoto K (2011) 14-3-3 proteins act as intracellular receptors for rice Hd3a florigen. *Nature* 476: 332-335

Google Scholar: [Author Only](#) [Title Only](#) [Author and Title](#)

The 1001 Genomes Consortium (2016) 1,135 genomes reveal the global pattern of polymorphism in *Arabidopsis thaliana*. *Cell* 166: 481-491.

Google Scholar: [Author Only](#) [Title Only](#) [Author and Title](#)

Tian L, Xie Z, Lu C, Hao X, Wu S, Huang Y, Li D, Chen L (2019) The trehalose-6-phosphate synthase TPS5 negatively regulates ABA signaling in *Arabidopsis thaliana*. *Plant Cell Rep* 38: 869-882

Google Scholar: [Author Only](#) [Title Only](#) [Author and Title](#)

Turck F, Fornara F, Coupland G (2008) Regulation and identity of florigen: FLOWERING LOCUS T moves center stage. *Annu Rev Plant Biol* 59: 573-594

Google Scholar: [Author Only](#) [Title Only](#) [Author and Title](#)

Van Dijck P, Mascorro-Gallardo JO, De Bus M, Royackers K, Iturriaga G, Thevelein JM (2002) Truncation of *Arabidopsis thaliana* and *Selaginella lepidophylla* trehalose-6-phosphate synthase unlocks high catalytic activity and supports high trehalose levels on expression in yeast. *Biochem J* 366: 63-71

Google Scholar: [Author Only](#) [Title Only](#) [Author and Title](#)

van Dijken AJ, Schluemann H, Smeekens SC (2004) *Arabidopsis* trehalose-6-phosphate synthase 1 is essential for normal vegetative growth and transition to flowering. *Plant Physiol* 135: 969-977

Google Scholar: [Author Only](#) [Title Only](#) [Author and Title](#)

Van Leene J, Eeckhout D, Gadeyne A, Matthijs C, Han C, De Winne N, Persiau G, Van De Slijke E, Persyn F, Mertens T, Smagghe W, Crepin N, Broucke E, Van Damme D, Pleskot R, Rolland F, De Jaeger G (2022) Mapping of the plant SnRK1 kinase signalling network reveals a key regulatory role for the class II T6P synthase-like proteins. *Nat Plants* 8: 1245-1261

Google Scholar: [Author Only](#) [Title Only](#) [Author and Title](#)

Vandesteeene L, López-Galvis L, Vanneste K, Feil R, Maere S, Lammens W, Rolland F, Lunn JE, Avonce N, Beeckman T, Van Dijck P (2012) Expansive evolution of the trehalose-6-phosphate phosphatase gene family in *Arabidopsis*. *Plant Physiol* 160: 884-896

Google Scholar: [Author Only](#) [Title Only](#) [Author and Title](#)

Wahl V, Ponnu J, Schlereth A, Arrivault S, Langenecker T, Franke A, Feil R, Lunn JE, Stitt M, Schmid M (2013) Regulation of flowering by trehalose-6-phosphate signaling in *Arabidopsis thaliana*. *Science* 339: 704-707

Google Scholar: [Author Only](#) [Title Only](#) [Author and Title](#)

Wang M, Zang L, Jiao F, Perez-Garcia M-D, Ogé L, Hamama L, Le Gourrierec J, Sakr S, Chen J (2020) Sugar Signaling and Post-transcriptional Regulation in Plants: An Overlooked or an Emerging Topic? *Front Plant Sci* 11: 578096

Wang Q, Sajja U, Rosloski S, Humphrey T, Kim MC, Bomblies K, Weigel D, Grbic V (2007) HUA2 caused natural variation in shoot morphology of *A. thaliana*. *Curr Biol* 17: 1513-1519

Google Scholar: [Author Only](#) [Title Only](#) [Author and Title](#)

Weigel D, Nilsson O (1995) A developmental switch sufficient for flower initiation in diverse plants. *Nature* 377: 495-500

Google Scholar: [Author Only](#) [Title Only](#) [Author and Title](#)

Wigge PA, Kim MC, Jaeger KE, Busch W, Schmid M, Lohmann JU, Weigel D (2005) Integration of spatial and temporal information during floral induction in *Arabidopsis*. *Science* 309: 1056-1059

Google Scholar: [Author Only](#) [Title Only](#) [Author and Title](#)

Xing LB, Zhang D, Li YM, Shen YW, Zhao CP, Ma JJ, An N, Han MY (2015) Transcription Profiles Reveal Sugar and Hormone Signaling Pathways Mediating Flower Induction in Apple (*Malus domestica* Borkh.). *Plant Cell Physiol* 56: 2052-2068

Google Scholar: [Author Only](#) [Title Only](#) [Author and Title](#)

Yadav UP, Ivakov A, Feil R, Duan GY, Walther D, Giavalisco P, Piques M, Carillo P, Hubberten HM, Stitt M, Lunn JE (2014) The sucrose-trehalose 6-phosphate (Tre6P) nexus: specificity and mechanisms of sucrose signalling by Tre6P. *J Exp Bot* 65: 1051-1068

Google Scholar: [Author Only](#) [Title Only](#) [Author and Title](#)

Yan W, Chen D, Kaufmann K (2016) Molecular mechanisms of floral organ specification by MADS domain proteins. *Curr Opin Plant Biol* 29: 154-162

Google Scholar: [Author Only](#) [Title Only](#) [Author and Title](#)

Yoo SK, Chung KS, Kim J, Lee JH, Hong SM, Yoo SJ, Yoo SY, Lee JS, Ahn JH (2005) CONSTANS activates SUPPRESSOR OF OVEREXPRESSION OF CONSTANS 1 through FLOWERING LOCUS T to promote flowering in *Arabidopsis*. *Plant Physiol* 139: 770-778

Google Scholar: [Author Only](#) [Title Only](#) [Author and Title](#)

Zacharaki V, Ponnu J, Crepin N, Langenecker T, Hagmann J, Skorzinski N, Musialak-Lange M, Wahl V, Rolland F, Schmid M (2022) Impaired KIN10 function restores developmental defects in the *Arabidopsis* trehalose 6-phosphate synthase1 (*tps1*) mutant. *New Phytol* 235: 220-233

Google Scholar: [Author Only](#) [Title Only](#) [Author and Title](#)